Breakup of Pangea and the Cretaceous Revolution

Xavier Le Pichon[1], A.M. Celal Şengör[2], Mark Jellinek[3], Adrian Lenardic[4] and Caner İmren[5]

[1]Collège de France, Paris, France

[2]İstanbul Teknik Üniversitesi, Maden Fakültesi, Jeoloji Bölümü ve Avrasya Yerbilimleri Enstitüsü, Ayazağa 34469 İstanbul, Turkey

[3]University of British Columbia, Department of Earth, Ocean, and Atmospheric Sciences, Vancouver, Canada

[4]Rice University, Department of Earth Science, Houston, TX, USA

[5]İstanbul Teknik Üniversitesi, Maden Fakültesi, Jeofizik Bölümü, Ayazağa 34469 İstanbul, Turkey

Corresponding Author : Xavier Le Pichon (xavier.lepichon@academie-sciences.fr)

Key Points:

- 250 to 100 Ma, oscillations of Pangea about itself triggered three successive phases of breakup
- The disruption of the subduction girdle of Pangea allowed lateral mixing and return to a globally homogeneous upper mantle
- The Cretaceous Revolution marked the passage 100 Ma from Pangea style tectonics to plate tectonics as we know it today

Abstract

250 Ma, Pangea had just reached an equatorial position of dynamic equilibrium, after a 60° northward migration due to True Polar Wandering. It then began oscillating about itself for the next 150 Myr. The resulting extensional stresses triggered three successive phases of breakup, controlled by the mechanical resistance of a crescent of thick lithosphere, surrounding the Tethyan realm, which had adjusted the supercontinent to its hemispheric shape. The fracturing of the crescent was produced in three successive generations, each new generation corresponding to Coulomb fractures, conjugates of the preceding set. Flood basalts were associated with these deep fractures within the thick lithosphere crescent. We consider unlikely that this highly ordered pattern of fracturing was determined by the locations of the impacts of successive plumes. Between 260 and 180 Ma, thermal isolation was maximal and the asthenosphere of Pangea was about 150°C warmer than below Panthalassa. From 180 to 100 Ma, the breakup elongated Pangea by about 3 000 km in a NNW-SSE direction, producing gaps in the subduction girdle. Lateral mixing began, leading to a continuous rise in global sea level and progressive return to a globally homogeneous upper mantle with sea-level at its maximum 100 Ma. This Cretaceous Revolution marked the end of the Pangea tectonics, radically different from our present plate tectonics.

Neither post-Cretaceous plate kinematic inferences, nor mantle dynamic and associated planetary cooling inferences are extendable to Pangea times.

1. Introduction

In this paper, we deal with the breakup of Pangea and its hemispheric girdle from its first manifestations 250 Ma to its disruption 100 Ma. Figure 1 shows the association between Pangea migration to the equatorial area, its oscillations about its axis and variations of global sea level and Figures 3 to 6 show the evolution from 220 Ma to Present. Figure 2 shows the 200-Ma reconstruction. We use a Lambert equal area projection of the totality of the Earth which permits a quantitative visual evaluation of the misfit of Pangea to a polar hemisphere (Le Pichon and Huchon, 1984). The reconstructions are from Müller et al. (2016), as are also all those used in this paper following Le Pichon et al. (2019a) and Le Pichon et al. (2021, called Le Pichon for short). Such reconstructions are model dependent and may differ significantly about the configuration of plate boundaries. For example, Müller et al. (2016) do not have a subduction zone dipping under the Cimmerian Continent (Figures 2 and 3) while a north Cimmerian subduction zone was active until its final collision with Laurasia for Şengör and Atayman (2009, see Figure 12a). However, recent reconstructions have a broad agreement on the relative positions of continental masses for the post-Paleozoic time. The reader should be aware of the significantly larger degree of uncertainty of the Paleozoic reconstructions.

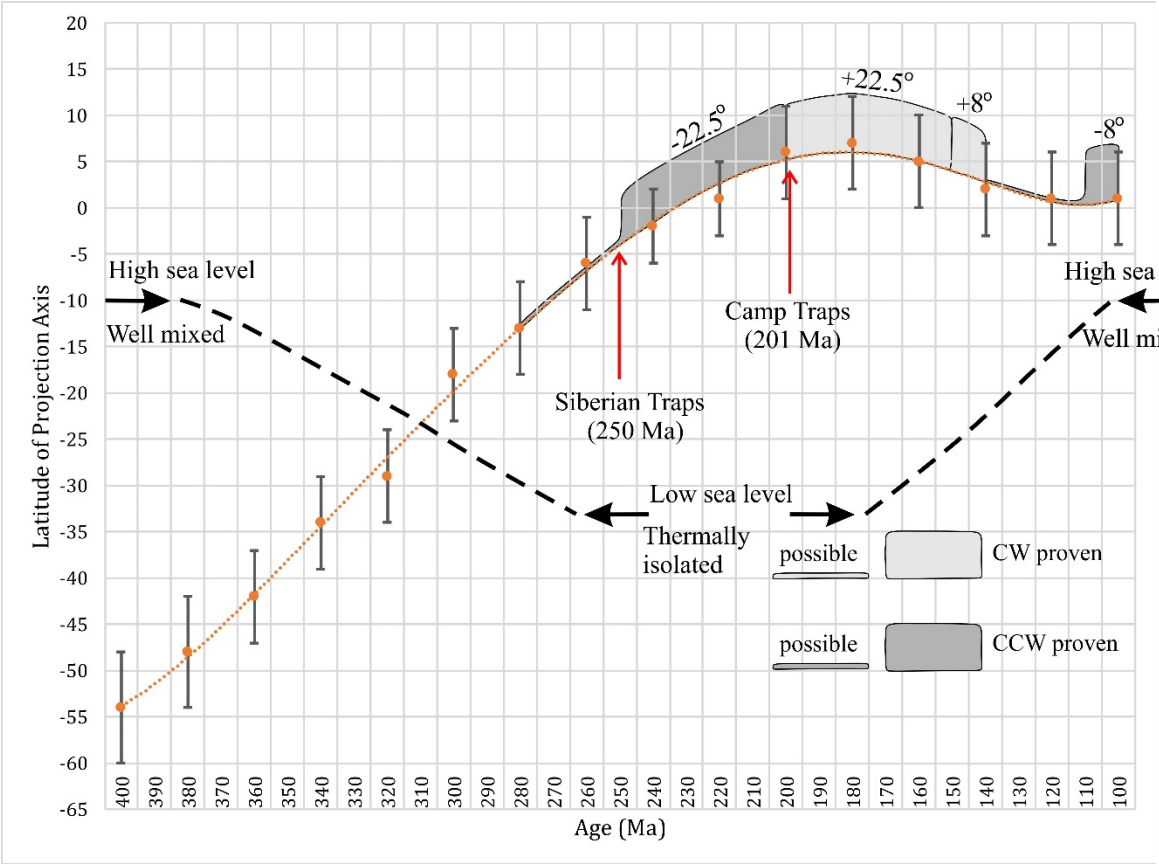

Figu

1. Latitude of projection of the axis of symmetry of the Pangea hemisphere versus time between 400 and 100 Ma at 20 Myr interval after Le Pichon et al. (2021). The counterclockwise (CCW) and clockwise (CW) rotations that affected Pangea during its migration are after Torsvik et al. (2012). The dates of the Siberian and CAMP traps coincide with the beginning and end of the first large CCW rotation of Pangea. The dashed black line shows in a schematic and qualitative fashion the long-term evolution of global sea level. There is a consensus to consider that a high sea level existed 400 Ma, a low sea level between 260 and 180 Ma, and high sea level again in Upper Cretaceous near 100 Ma so that long-term sea level trend was decreasing between 400 and 260 Ma and rising between 180 and 100 Ma (Miller et al., 2005; Snedden & Liu, 2010).

Following Le Pichon, we consider that Pangea existed when all continental material was contained within a hemispheric subduction girdle. We build on the results of a series of papers (Le Pichon and Huchon, 1983, 1984; Le Pichon et al., 2019a; Le Pichon) which proposed that Pangea had a tectonic environment radically different from our present plate tectonic one. Le Pichon argued, follow-

ing Le Pichon et al. (2019a), that Pangea was stationary or moved very little with respect to the mantle because the subduction girdle hampered significant lateral motion as well as lateral mixing in the upper mantle. This effect, in turn, resulted in an increase in mantle temperature below the thick, stagnant, and mostly continental lithosphere of the Pangea hemisphere and a corresponding decrease below the thinner oceanic lithosphere of the Panthalassa hemisphere, while the average temperature of the whole mantle would have stayed constant (Lenardic et al., 2011). The distribution of masses associated with Pangea was such that it reached a position of dynamic equilibrium about 250 Ma when its axis of symmetry became equatorial after Pangea had migrated about 60° northward between 400 and 250 Ma through True Polar Wandering (TPW) (Le Pichon) (see Figure 1). The subject of this paper concerns the 250-100 Ma period, during which Pangea, that was finishing its final stage of assembly and had just reached a position of dynamic equilibrium, with its axis within the equatorial plane, entered a process of disruption of the subduction girdle that allowed lateral mixing and return to a globally homogeneous upper mantle. Le Pichon proposed to call such a continent a Buridanian continent and Le Pichon and Huchon (1984) called Cretaceous Revolution the passage about 100 Ma from Pangea style tectonics to plate tectonics as we know it today.

We follow Le Pichon et al. (2019a) and Le Pichon and use global sea level as a first order reliable indicator of the thermal state of the upper mantle below the lithosphere during Pangea time as predicted by the model of Lenardic et al. (2011). As just discussed, the stationarity of Pangea, imposed by its surrounding curtain of slabs down to at least 400 km depth, led to thermal isolation and subsequent warming of the sub-Pangean mantle and cooling of the sub-Panthalassa mantle. Over time, the resulting lateral thermal gradients from relatively warm sub-Pangea mantle to cooler sub-oceanic mantle destabilized the Pangea landmass and its associated subduction girdle with breakup of Pangea and thermal homogenization of the global mantle. As a result, global sea level was high when the global upper mantle was thermally homogeneous and low when it was thermally isolated. To first order, sea level was high before the assembly of Pangea 400 Ma and was low between 260 and 180 Ma when it was fully assembled in the equatorial region (Figure 1). Then sea level increased again between 180 and 100 Ma during the breakup of Pangea to reach another maximum after 100 Ma as thermal homogenization of the global mantle had been completed. We investigate the breakup of Pangea between 250 and 100 Ma and show how it accounts for the rise in sea level from 180 to 100 Ma. We show that the breakup was controlled by the mechanical resistance of the thick cold lithosphere that formed the armor of Pangea. The breakup between 180 and 100 Ma elongated Pangea by about 3 000 km in a NNW-SSE direction. This elongation produced gaps in the subduction girdle. We argue that, between 260 and 180 Ma, thermal isolation was maximal, that progressive thermal homogenization began during breakup and that complete thermal homogenization had been reached 100 Ma.

1) We describe the structure of the crescent shaped thick lithosphere, surrounding the triangular Tethyan oceanic realm, which formed the armor of Pangea.

We show that the distribution of lithosphere is such that the Tethyan realm acted as an escape hatch for the sub-Pangea asthenosphere. 2) We explicit the reasons why Pangea was a unique tectonic object. 3) We analyze the kinematics of the breakup. 4) We consider the pattern of fracturing of Pangea between 180 Ma and 100 Ma and show that it was governed by the mechanically coherent breakup of the crescent of thick lithosphere that formed the armor of Pangea. 5) We investigate the process of formation and consolidation of the thick lithosphere crescent. 6*)* We describe the extensional phases that led to the breakup of Pangea. 7) We explore the significance of the Cretaceous Revolution that marked the transition from Pangea tectonics to contemporaneous plate tectonics. 9) The last section provides a general discussion and conclusion.

1. **Lithospheric structure of Pangea**

Figure 2 shows the lithospheric thickness distribution after McKenzie et al. (2015) who adopted the estimations made by Priestley and McKenzie (2013) for present Earth and assumed that the present lithosphere thickness had not changed significantly through time. They used Rayleigh wave tomography to determine the temperature as a function of depth, and hence the lithospheric thickness, by fitting a geotherm to temperature estimates $> 900°C$ at depths >100 km. However, they removed thick lithosphere associated with present active continental shortening as well as the large values along the Pacific margin of South America that result from the high velocity in the subducting slab. McKenzie and Priestley (2008) had mapped in this way areas of thick continental lithosphere using surface wave tomography and had discovered that these areas do not consist only of Precambrian shields. Although Precambrian shields are present, they are now parts of larger regions of continuous thick lithosphere. They pointed out further that they were highly resistant to deformation, especially shortening. They proposed that their strength principally resides in their dry crust, which remains relatively cold because it is insulated from the convecting mantle by a thick layer of low density harzburgite.

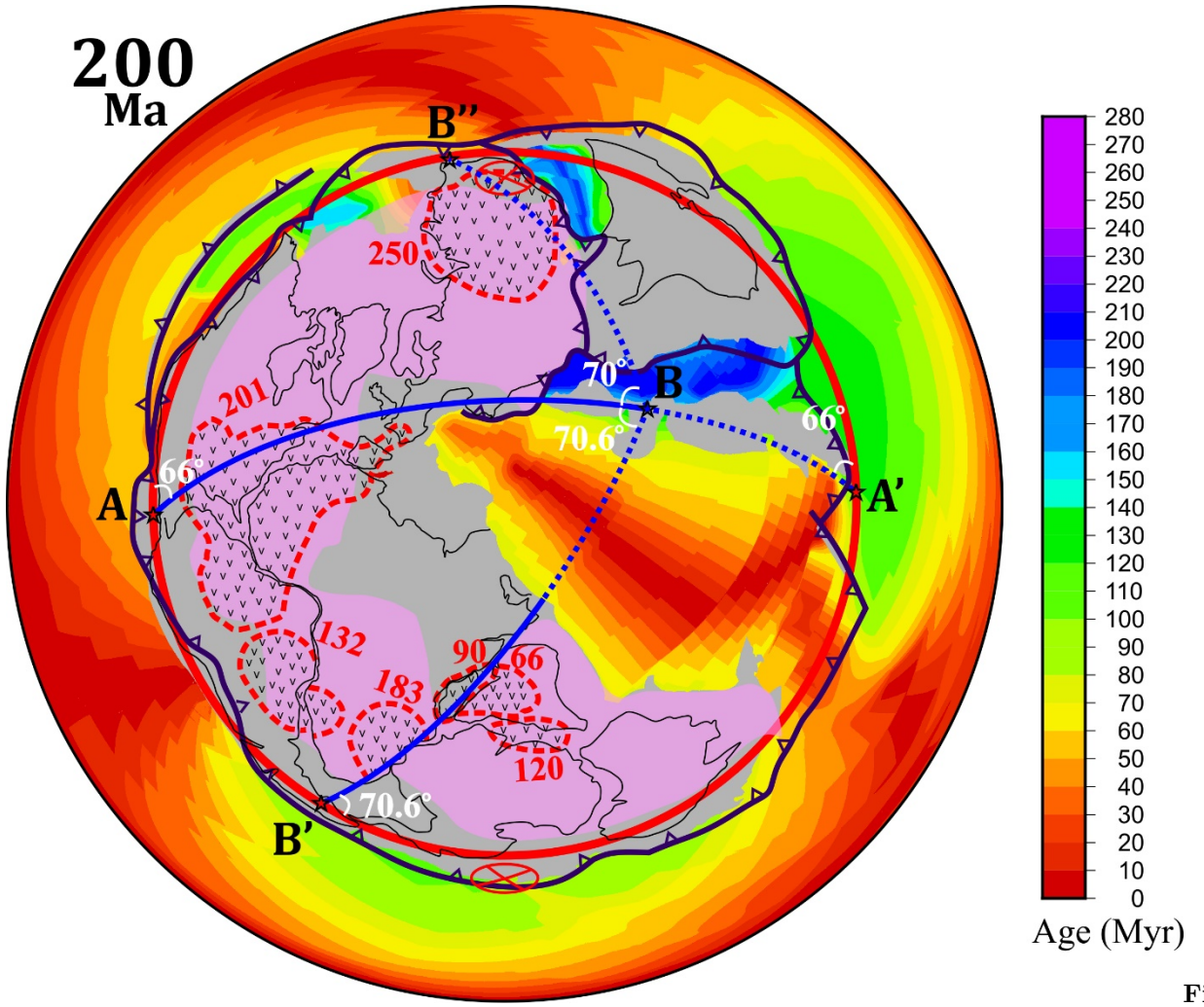

Figu

2. The early fracturation of Pangea. 200 Ma reconstruction of Müller et al. (2016). Lambert Azimuthal Equal Area projection with pole of projection at 8°N, 34°E that best fits the Pangea hemisphere. The upper hemisphere is projected unto the equatorial plane of projection within the first great circle. The hidden hemisphere is shown distorted beyond the great circle (thick red line). Symbols ( ) in red show locations of north and south poles. The main subduction zones are shown in black. Pink indicates area of thick continental lithosphere after McKenzie et al. (2015, see text)). "v pattern" surrounded by dashed red line indicates maximum extent of flood basalt provinces with age in red (see text). Continuous blue lines are great circles fitted to the major fractures affecting Pangea. Dashed blue lines are continuations of great circles (see text). Centers of great circles of AA', BB' and BB'' are 65°S, 38°E; 30°S, 146°E; and 7°S, 18°W, respectively. The values of the angles between great

circles are given in degrees.

Figure 2 illustrates the observation made by McKenzie et al. (2015) that two thirds of Pangea consisted of a crescent-shape 3-4,000-km-wide backbone of very thick (260 to 150 km) lithosphere. This crescent was put into place during the collision of Laurasia to the north with Gondwana to the south. We will demonstrate that this backbone acted as an armor highly resistant to deformation. The remaining third of the Pangea continent was made of thin mechanically much less resistant lithosphere, fringing this crescent both outside and inside. On the outside, bordering the subduction zone, a 1-2,000-km-wide band of thin lithosphere was associated with the active margin of Pangea, comprising Phanerozoic mobile belts, including the Gondwanides of Keidel (1916), products of what Du Toit (1937) called the Samfrau geosyncline. On the inner side of the arc was another large area of thin and weak lithosphere. McKenzie (2020) confirmed that the present lithosphere there is indeed quite thin as its thickness is less than 70-50 km. Note that the area of weak lithosphere extends to the south to eastern Africa and Arabia which correspond to what Şengör et al. (2021) called the Saharides, a mobile belt affected by neo-Proterozoic deformation between 900 and 500 Ma. The 20% remaining space, surrounded by the crescent, was oceanic. It was occupied by the triangular relatively young Tethyan realm (less than 100 Myr old). Its lithospheric thickness did not exceed 80 km and was vanishingly small near the ridge crest.

The thickness of the lithosphere of Pangea thus progressively increased from very little at the crest of the ridge within the Tethyan realm to more than 150 km and up to 260 km within the thick cold surrounding continental lithospheric crescent. This had two consequences. First, as just stated above, the Pangea lithosphere formed a crescent shape mechanically strongly resistant armor, open to the east where thin oceanic Tethyan lithosphere was in direct contact with the subduction girdle. As we will demonstrate later, this mechanically strong crescent controlled the resistance to the breakup. Second, the funnel shape opening to the east resulted in the Tethyan realm collecting the heat and magma from the asthenosphere below the surrounding continental Pangea and acting as a large escape hatch where heat and magma could vent out. On the other hand, any asthenospheric material from Panthalassa, above the 250-260 km level, that may have gone through the subduction girdle during the breakup phase, was blocked by the keel of the thick lithosphere crescent and consequently could only reach the inner part of Pangea through the eastern portion of the Tethyan realm. Le Pichon et al. (2019a, 2019b) proposed that this lithospheric structure accounts for the gradation in tectonics from the thick lithosphere of the backbone of Pangea with large-scale rifts and flood basalt outpourings, such as in the CAMP and Siberian magmatic provinces, to the thin and hot continental lithosphere with mostly alkalic and calc-alkalic volcanism and plastic-like material behavior bordering the Tethyan oceanic realm.

Finally, Figure 2 shows the approximate maximal extent of the large magmatic provinces produced by flood basalt during the fracturing of Pangea. These

flood basalts erupted exclusively over the thick lithosphere backbone area. Le Pichon et al. (2019a) and Le Pichon interpreted this remarkable observation in the following way. The asthenosphere below Pangea was about 100° to 150°C warmer than normal asthenosphere (Lenardic et al., 2011) and partial fusion was expected, increasing as the asthenosphere became shallower toward the the Tethyan realm. In addition, plume material accumulated within this hot asthenosphere. Under the thinner lithospheric zones surrounding the Tethyan realm, partially fused material was funneled toward the ocean where it could be evacuated in accreting and consuming boundaries before large accumulations could occur. In contrast, below the thick cold lithosphere, where the top of the asthenosphere is significantly deeper, massive melting only occurred after fracturing, within the material rising in the fractures, producing the extensive flood basalt provinces (White & McKenzie, 1995; see also Şengör & Atayman, 2009).

1. **Pangea: a unique tectonic object**

Supercontinents have been present over the Earth during approximately one half of its existence (Paulsen et al., 2022). It is becoming increasingly clear that geodynamics is significantly affected by the presence of a supercontinent. Multiple proxy data sets suggest that lows in crustal recycling and thickness are associated with the presence of a supercontinent whereas highs are associated with the breakup of the supercontinent (Paulsen et al., 2022). The assembly of a supercontinent has been shown to have the potential to slow down plate motions and reduce global cooling whereas warming caused by the insulating effect of a supercontinent could provide an added driver of mantle flow and plate motions (Lenardic, 2017). Here we want to examine more thoroughly what made unique the tectonics of Pangea, the last and best known supercontinent.

1. **Unique kinematics**

Pangea was enclosed within a subduction girdle that corresponded exactly to a great circle (Le Pichon and Huchon, 1983, 1984, Figure 2). Because the total volume and total surface of the continents over the Earth have changed only very slowly through time (e.g. Cawood et al., 2013), we can ignore changes that occurred during the last 300 Myr and deduce that the Pangea continent occupied 80% of the surface of the hemisphere and that the remaining 20% were occupied by oceanic space. In this paper, we call this oceanic space the Tethyan realm. It was occupied by successive oceans that geologists have called Paleo-Tethys and Neo-Tethys. The reconstructions further indicate that this space was equatorial and triangular with its apex to the west. Any kinematic change within Pangea could only occur either along the peripheral subduction zones with possible creation and destruction of marginal basins or through transfer of pieces of continent from one side of the Tethyan realm to the other side. Note that this transfer had the peculiarity to be a one-way transfer from south to north. As the oceanic surface had to stay constant within the Pangea hemisphere, any surface destroyed by subduction had to be compensated by surface formed by oceanic accretion. This powerful constraint applied to the Pangea plate tectonics which

was thus radically different from present plate tectonics.

1. **Asthenosphere temperature 100-150°C higher than normal leading to radial extension**

Because the subduction girdle hampered significant lateral motion as well as lateral mixing in the upper mantle, Pangea could not move significantly with respect to the mantle. As pointed out in the Introduction, this led to an increase in mantle temperature below the thick, stagnant, and mostly continental lithosphere of the Pangea hemisphere. Consequently, a second unusual character was the presence of a temperature higher than normal in the asthenosphere below the Mesozoic Pangea. The average temperature of the thermally isolated upper mantle below Pangea continuously increased and led to a gradual uplift of the continent. As noticed by many authors (e.g. Anderson, 1982, 1994; Coltice et al., 2007, 2009), such a continuous increase is inherently unstable. The resulting topographic bulge would tend to spread toward the peripheral subduction girdle. As a result, a radial component of extensional stress should have been present within Pangea and eventually contribute to the breakup of the subduction girdle and the dispersion of Pangea. The excess temperature had reached a value of about 100-150°C about 200 Ma (Lenardic et al., 2011, see discussion in Le Pichon). Because of the increase of the melting temperature with depth, partial fusion should have been much more present below thin lithosphere than below the 200-270 km cold lithosphere (see section 1 and Figure 2). Consequently, below the thick lithosphere crescent, partial fusion was rare. However, whenever fracturing of the base of the lithosphere occurred and material could come up within the fractures, massive melting would be expected (White and McKenzie, 1995). Inside the crescent, the depth of the base of the lithosphere decreased rapidly from 200-270 km in the crescent area to zero depth at the axis of rift in the Tethyan realm and unusually hot and light material tended to move toward it. As it moved up, partial melting increased and was rapidly evacuated through this oceanic space that acted as a venting system. This however was not true for the eastern part of what will become Asia which was separated by a subduction zone and its slabs from the Tethyan realm and therefore had no easy access to it.

1. **The arrival of Pangea within the equatorial zone at the origin of successive phases of circular extensional stresses**

Pangea reached a position of dynamic equilibrium about 250 Ma when its axis of symmetry became equatorial. An explanation for the formation of such a system may be given by the proposal by Zhong et al. (2007) that the supercontinent assembly may result from degree 1 planform convection. The supercontinent assembly then led to degree-2 planform convection with antipodal upwelling and consequent migration through True Polar Wander (TPW) to the equatorial location, which is its position of stability, as the associated geoid of order-2 had then its negatives centered on the poles and its positives on the equator (Zhong et al., 2007). Le Pichon proposed that the formation of Pangea itself could lead to a similar effect. This is because the initial formation of a subduction gir-

dle would lead to significant mass anomalies which, together with sub-Pangean thermal isolation (Jellinek et al., 2020; Lenardic et al., 2011), could provide the type of internal mantle loading that Creveling et al. (2012) argued could drive a TPW event that would bring Pangea to the equator.

As Pangea reached the equatorial zone, after its 60° northward migration, it began to oscillate about itself. Steinberger and Torsvik (2008) and Torsvik et al. (2012) showed that, between 250 and 220 Ma, the arrival of Pangea within the equatorial zone was accompanied by a large (22.5°) CCW rotation about its axis. The CCW rotation was followed by a CW one of similar amplitude during the return to the equator (200-160 Ma). A second set of similar but twice smaller rotations occurred between 160 and 100 Ma (Figure 1). These authors considered the rotations as TPW and corrected for them. Creveling et al. (2012) also interpreted this set of successive rotations as TPW and considered them to be part of a 150 Myr long oscillation (250 to 100 Ma) driven by an elastic restoring force arising in response to memory of Earth's rotational bulge. Le Pichon pointed out that the initiation and reversal of rotations were times of major change in elastic stresses within the lithosphere. We do not know how long lasted the phase of change from no rotation to rotation, neither from a reversal of rotation. The shorter the phase, the larger the strain imposed. Unfortunately, the paleomagnetic information is not precise enough to give this information. But we can conclude that the arrival of the Earth in its dynamic equilibrium zone as the axis of rotation reached the equatorial plane led to substantial extensional stresses. We attempt in this paper to show that they played an essential role in the breakup of the Pangea thick lithosphere armor.

The expected major disruptions in the pattern of stresses should thus have happened during the first CCW rotation initiation centered on 250 Ma, during the change from CCW to CW centered on 200 Ma and during the progressive change from CW to CCW between 140 and 110 Ma (Figure 1). We will show that, during each of these three phases of change in the oscillations of Pangea, not only major fracturing occurred but that fracturing was often accompanied by flood basalt eruption.

1. **Kinematics of breakup**

We now investigate the kinematics of the breakup. Although the first signs of widespread extension began near the end of Permian 250 Ma, the breakup only became evident in the kinematics 180 Ma. Figures 3, 4, 5 and 6 show the progression of the breakup of the continental hemisphere between 220 Ma and Present. We make a quantitative estimate of the change between 200 and 80 Ma, although one should be aware that this estimate is model dependent and that it implies significant uncertainties that are difficult to evaluate. Pangea was progressively elongated in a 20°W-160°E direction by about 1900 km to the north and 1100 km to the south transforming the great circle in a spherical ellipse with the large axis about 23 000 km long whereas the short axis kept its original length of 20 000 km, resulting in a 15% lengthening of the long axis. The total increase in surface of Pangea was also about 15%. This increase

was entirely due to oceanic surface formation which nearly doubled in surface, so that the proportion of Pangea occupied by oceanic space, in the Tethyan realm as well as in new oceanic spaces, increased from one fifth to about one third. A remarkable result of this breakup of Pangea is that the outgrowth over Panthalassa is obtained by migration of continent along the two NNW and SSE extremities of the spherical ellipse whereas the actual increase in surface is obtained by formation of new oceanic space by dislocation of Gondwana-Land within the median portion of the elongated Pangea (see 100 and 80 Ma reconstructions in Figure 4). This implied the advection of a large amount of asthenospheric material from Panthalassa below the median portion of Pangea contributing to the global thermal homogenization of the asthenosphere.

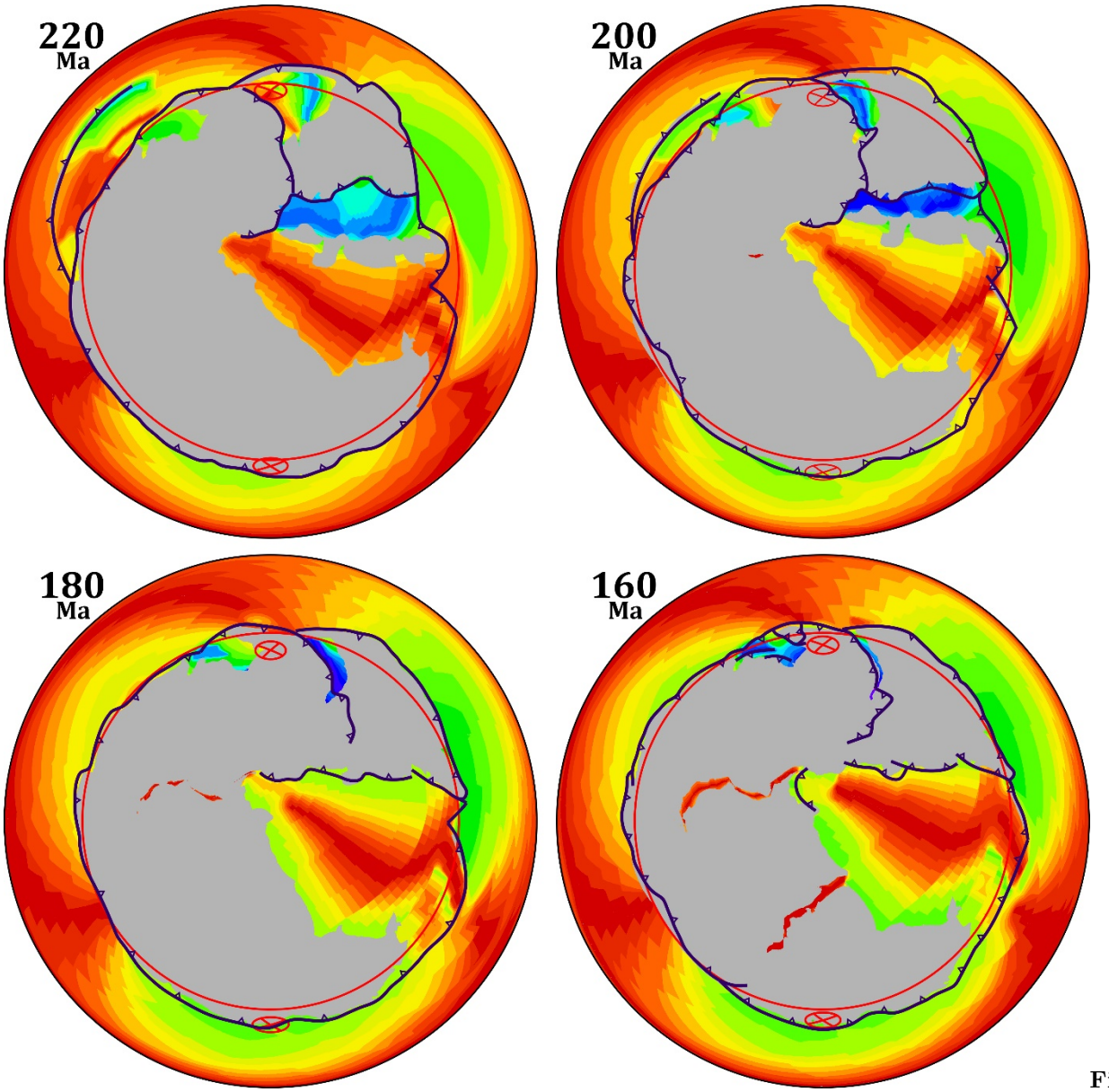

Figu

3. Müller et al. (2016) 220 Ma to 160 Ma reconstructions modified from Le Pichon et al (2019a). Lambert Azimuthal Equal Area projection with poles of projection at 4°N, 35°E; 8°N, 34°E; 10°N, 34°E; and 7°N, 34°E for the ages 220, 200, 180, and 160 Ma, respectively.

But how did the asthenospheric material of Panthalassa penetrate within the upper mantle of Pangea? Let us consider the increase in length of the subduction girdle. This is important as the subduction girdle was responsible for the

thermal insulation of the sub-Pangea mantle. The length of the subduction girdle increased from about 40 000 km (length of great circle) to about 45 000 km. This lengthening occurred mostly through the formation of three new oceanic spaces that will become the Caribbean and Southern Caribbean on the west side and a new Tethyan opening on the southeast side. The gaps in the subduction girdle are model dependent and their actual configurations are difficult to reconstruct. However, the reconstructions lead us to conclude that the lengthening of the subduction girdle occurred through formation of these three oceanic gaps and not by distributed deformation within it, although coast parallel strike-slip faulting in the hinterland of the Andes is known to have occurred possibly until the Cretaceous. These gaps were situated at the three summits of the triangular median portion of Pangea now principally occupied by new oceanic area (Figure 4). Their positions indicate that they are tightly linked to the new distribution of oceanic space within the former disrupted Gondwana-Land. It seems logical to assume that they played the key role in the exchange of asthenospheric material between Panthalassa and Pangea. Figures 4 and 5 show that, beyond 100 Ma, the breakup of the girdle was sufficiently advanced to allow Antarctica-Australasia to move outward within Panthalassa (see the Panthalassa side on Figure 6 for 60-0 Ma) while the Tethyan realm was being closed.

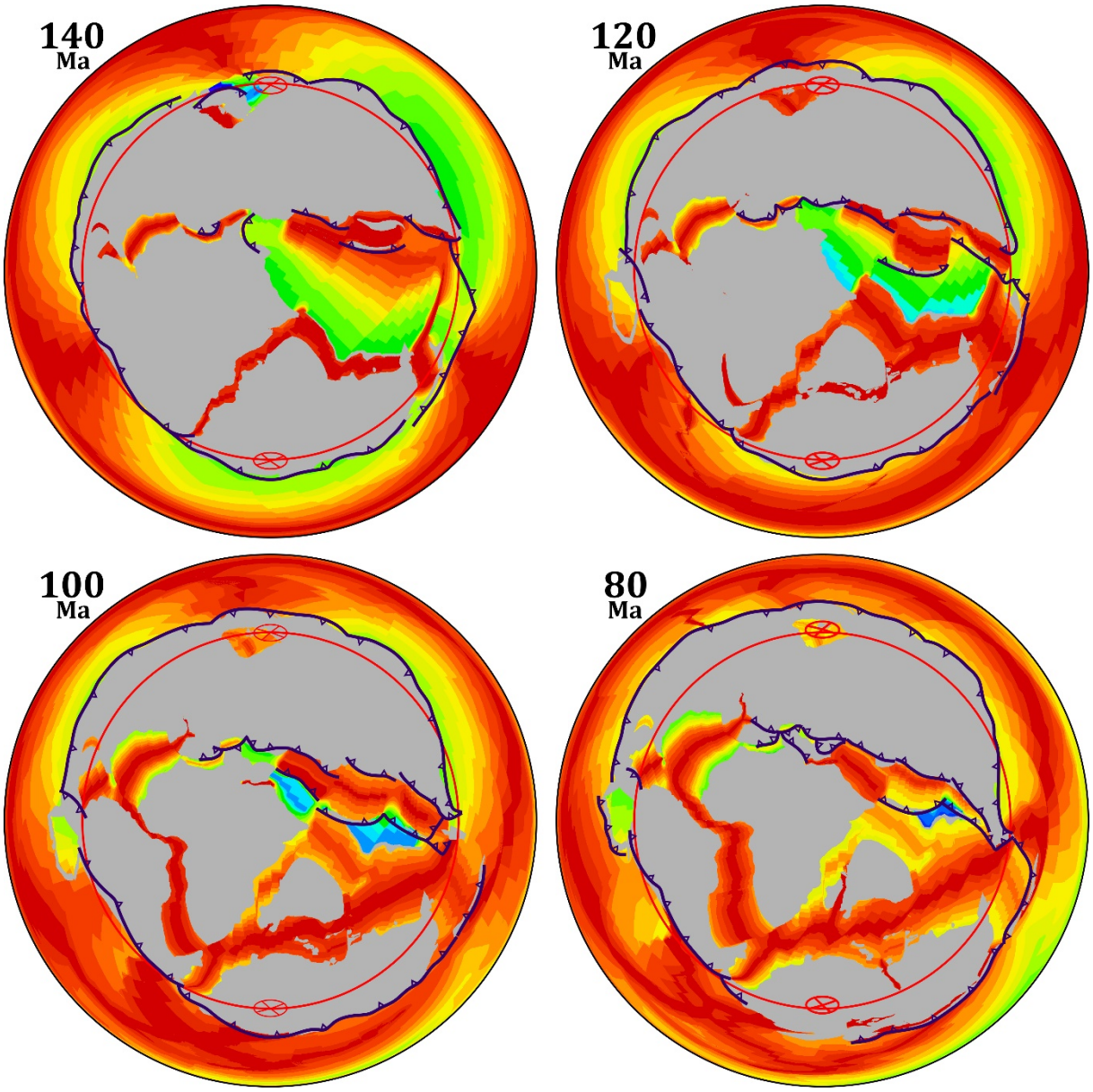

Figure 4. Müller et al. (2016) 140 Ma to 80 Ma reconstructions modified from Le Pichon et al (2019a). Lambert Azimuthal Equal Area projection with poles of projection at 1°N, 34°E; 1°N, 34°E; 0°N, 32°E; and 2°S, 30°E for the ages 140, 120, 100, and 80 Ma, respectively.

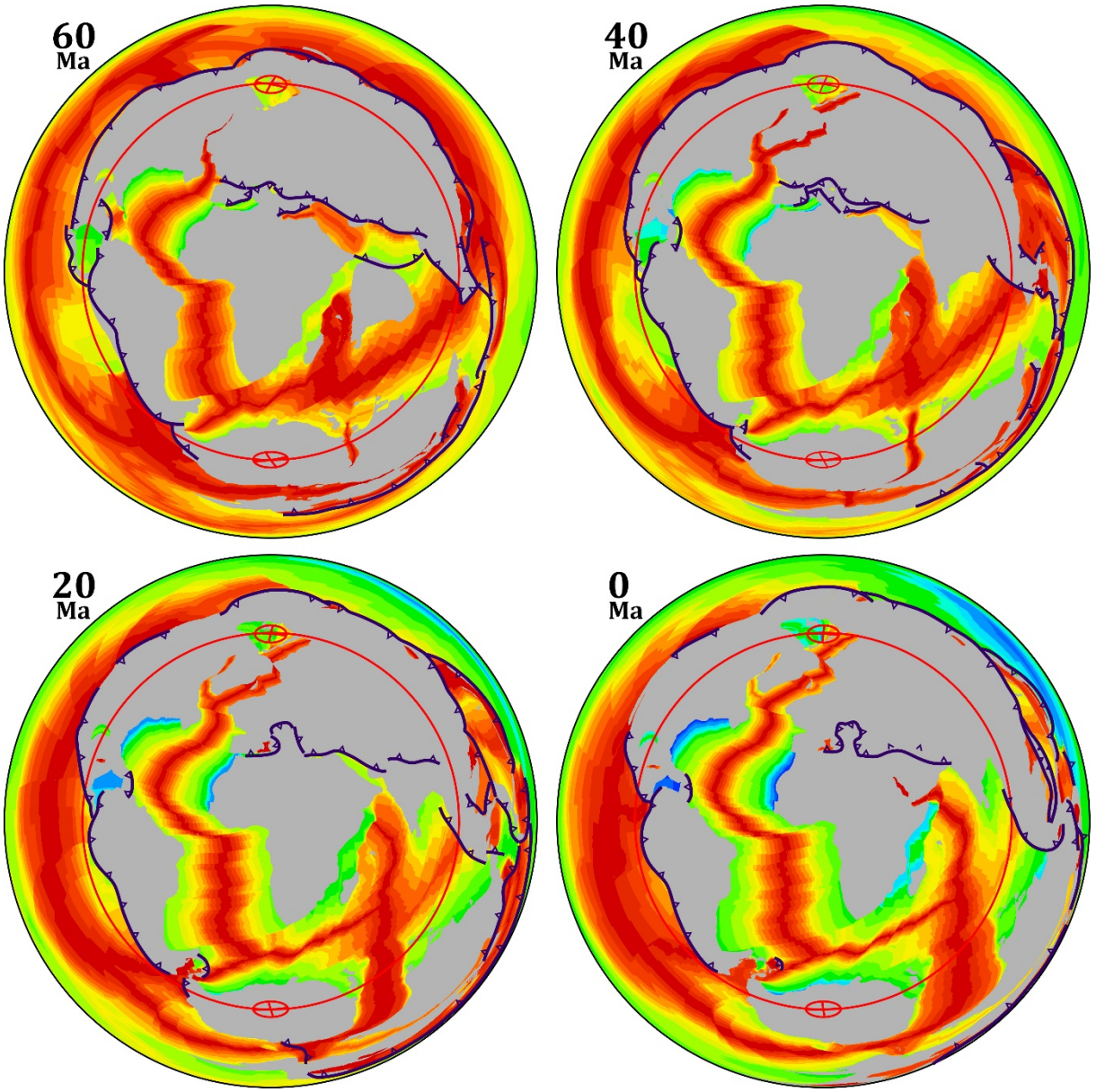

Figure 5. Müller et al. (2016) 60 Ma to Present reconstructions modified from Le Pichon et al (2019a). Lambert Azimuthal Equal Area projection with poles of projection at 6°N, 18°E; 6°N, 14°E; 6°N, 8°E; and 6°N, 4°E for the ages 60, 40, 20, and 0 Ma, respectively.

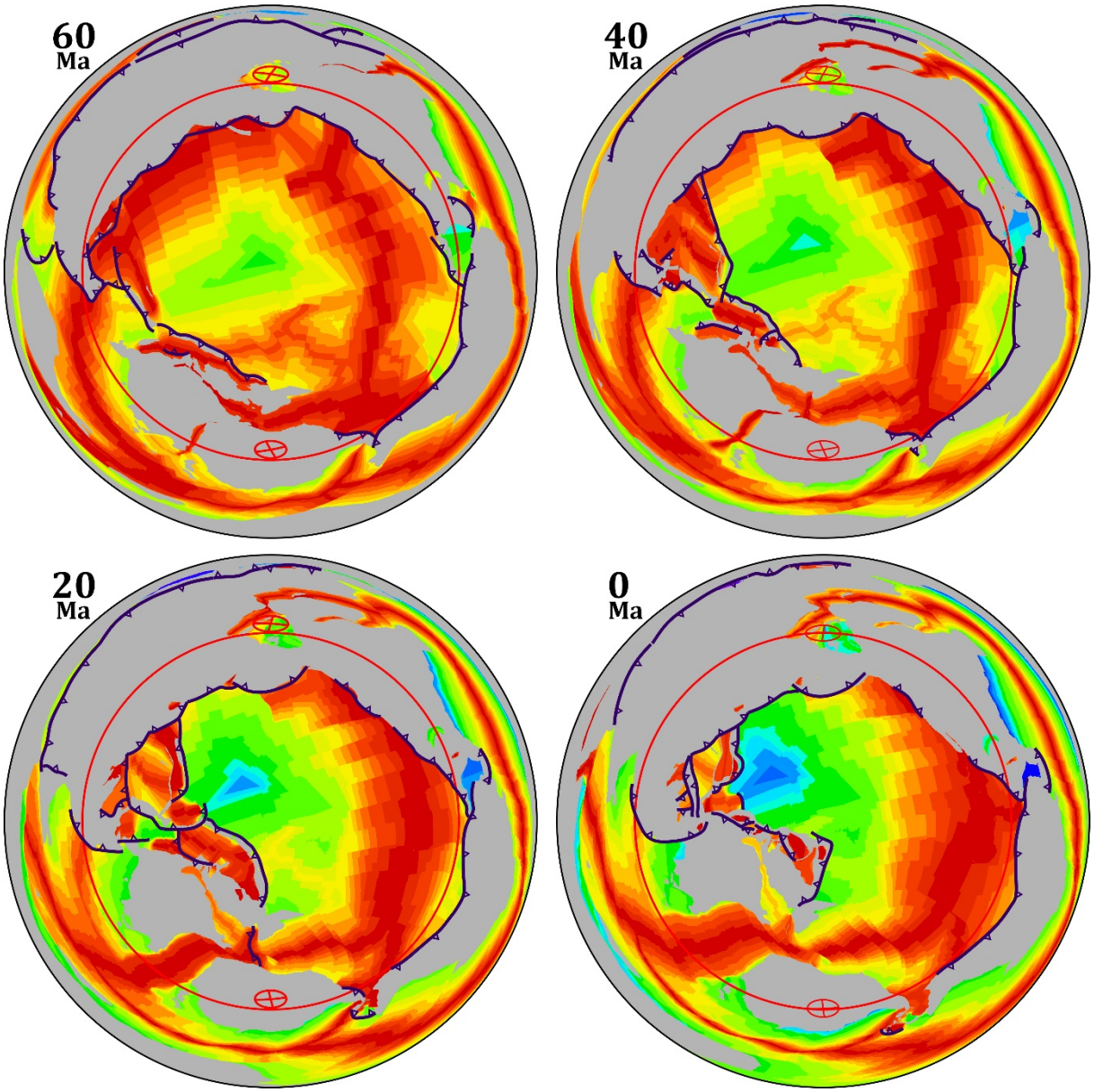

Figure 6. Same as Figure 5 centered on Pacific hemisphere. Lambert Azimuthal Equal Area projection with poles of projection at 6°S, 162°W; 6°S, 166°W; 6°S, 172°W; and 6°S, 176°W for the ages 60, 40, 20, and 0 Ma, respectively.

We now consider more precisely the kinematics of breakup of Pangea. The change in kinematics before and after 100 Ma is best seen in Figures 7a, 7b, (160 to 80 Ma) and 8a and 8b (60 to 0). The ingression of the America por-

tion of Laurasia within Panthalassa to the northeast (Figures 7a and 7b) was due to the clockwise rotation of Laurasia between 200 and 80 Ma about the average pole of rotation R1 along the northern border of the Tethyan realm, at the limit between eastern and western Tethys. Western Gondwana-Land, attached to southern Tethys, did not move significantly with respect to the mantle (Figure 7b). The R1 rotation of Laurasia resulted in the formation of a fracture between western Laurasia and Western Gondwana-Land that progressed westward forming oceanic space that will become the Central Atlantic and the Caribbean area. The motion of Laurasia away from Western Gondwana-Land was about 3 000 km (Gap1 in Figure 7b). As for Eastern Gondwana-Land, its motion clockwise obeyed approximately the same R1 rotation and was about 1500 km (Gap2 in Figure 7), producing a narrow oceanic space that separated it from Western Gondwana-Land. After 140 Ma, the kinematics changed as Eastern Gondwana-Land started to pivot counterclockwise about the average R2 pole situated in the future southern Caribbean and consequently also began to infringe on Panthalassa (Figure 7b). This motion produced an opening of about 2 500 km within Eastern Tethys (Gap3 in Figure 7b) but the actual change of the subduction girdle is highly model dependent.

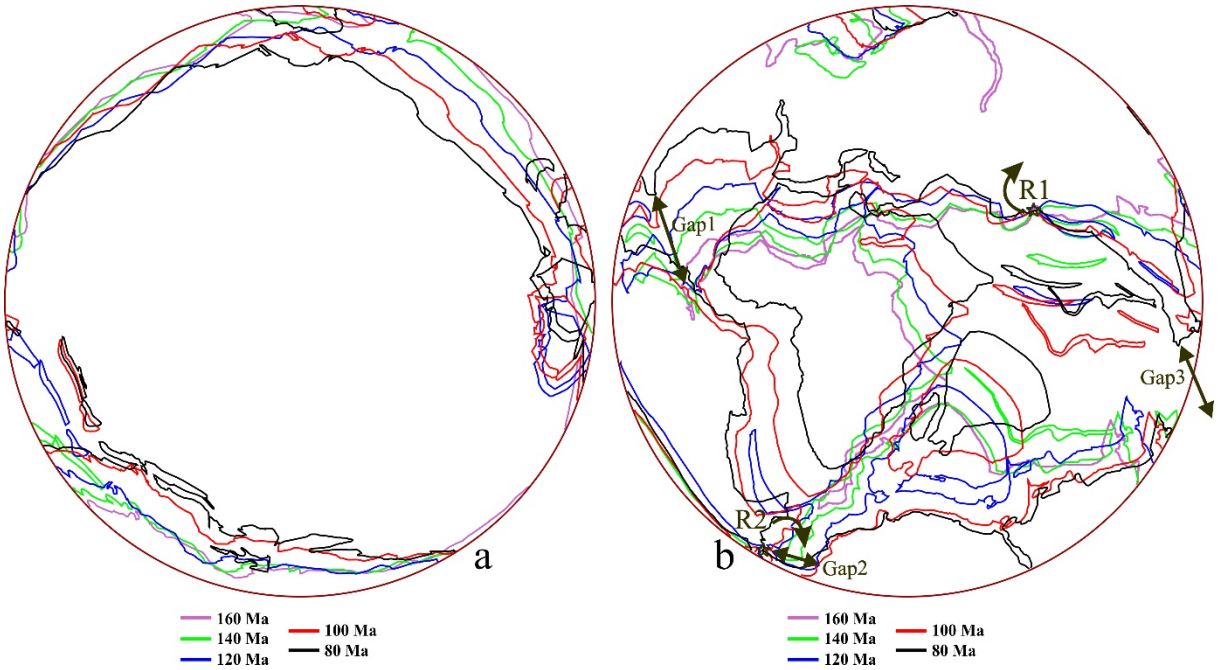

Figure 7. Contours of continents from 160 to 80 Ma at 20 Myr interval from the reconstructions presented in Figures 3, 4. a) Panthalassa hemisphere; poles of projection at 7°S, 146°W; 1°S, 146°W; 1°S, 146°W; 0°S, 148°W; and 2°N, 150°W for the ages 160, 140, 120, 100, and 80 Ma, respectively. b) Pangea hemisphere. R1, R2, respectively, poles of average rotation of Laurasia between 160 and 80 Ma and of Eastern Gondwana between 120 and 80 Ma. Gap1 and

Gap2 produced by R1, Gap3 by R2.

Finally, Figures 5, 6 and 8a show the dramatic change that occurred after 100 Ma. At this time, the subduction girdle had been widely breached to the east and thermal homogenization was sufficiently advanced that nothing prevented Australasia to fully move within southwestern Panthalassa. Pangea, as a Buridanian continent, ceased to exist about 100 Ma. This dispersion stage, the Cretaceous Catastrophe of Le Pichon and Huchon (1984), occurred in Aptian-Albian time during Early Cretaceous. It resulted in an encroachment of about one third of the surface of Pangea over Panthalassa, accompanied by the development of marginal basins.

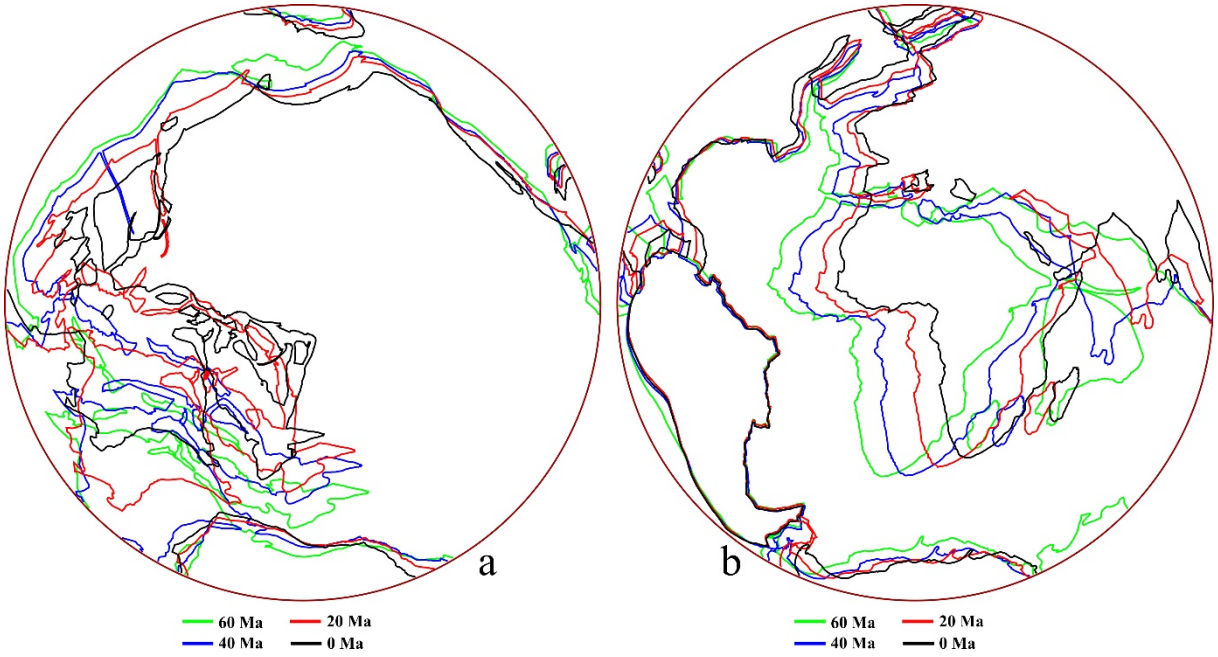

Figure 8. Same as Figure 7 for 60 Ma to Present. Pole of projections are same as Figures 5 and 6. a) Panthalassa hemisphere b) Pangea hemisphere. In b), South America has been fixed to obtain motions with respect to it. The comparison of Figures 7a and 8a illustrates the dramatic change that occurs during the post-100 Ma dispersal.

1. **Fracturing of Pangea**

We next consider the fracturing of Pangea between 200 and 100 Ma to help elucidate the nature of the forces that acted to produce its breakup. As discussed in section 2, a crescent shaped 3-4,000-km-wide crescent of strong thick (260 to 150 km) lithosphere occupied about two thirds of the continental space (Figure 2, Figure 12b). Elsasser (1967) pointed out that the lithosphere acts as a stress guide because stresses rapidly dissipate within the weak asthenosphere. Elsasser was considering the vertical rheological stratification from lithosphere

to asthenosphere. Here, we deal with horizontal juxtaposition of strong and weak lithosphere. In both cases, stresses rapidly dissipate within the underlying or adjacent weak zone and, as a result, the strong lithosphere concentrates the stresses and acts as a stress guide. We will show that, within Pangea, the strong thick continuous lithospheric crescent concentrated the stresses due to the forces acting to disrupt Pangea. During a first extensional phase between 250 and 140 Ma, the stress pattern was a remarkably homogeneous circular extension within the thick lithosphere crescent. By 140 Ma (Figure 9), this extension had resulted in the formation of three blocks: Laurasia, Western and Eastern Gondwana-Land. During the second phase of disruption, between 140 and 100 Ma (Figures 10 and 11), the pattern changed to one of progressive extensional fragmentation of Eastern and Western Gondwana-Land.

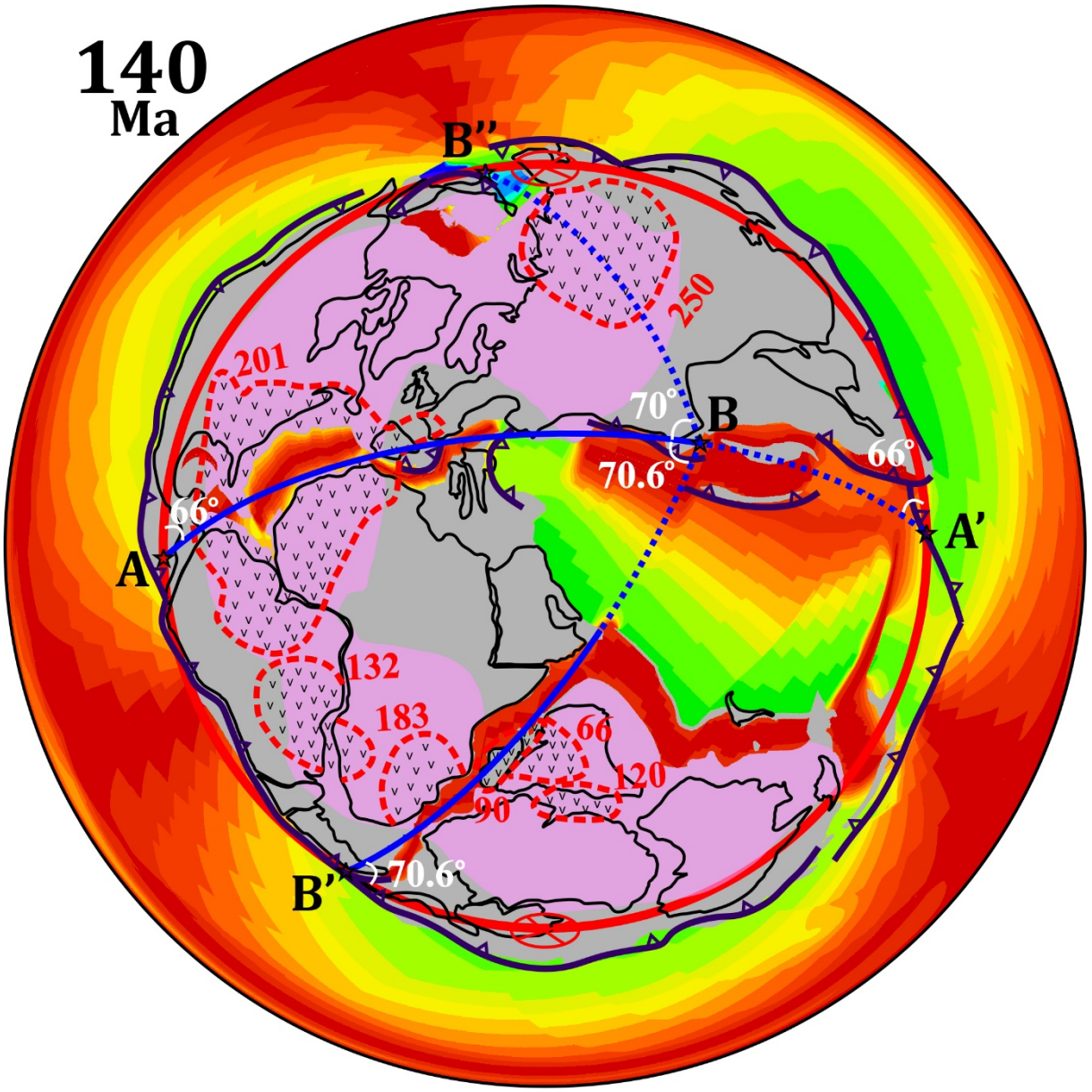

Figure 9. Fracturation of Pangea on 140 Ma reconstruction. Lambert Azimuthal Equal Area projection with pole of projection at 1°N, 34°E. Centers of great circles of AA', BB' and BB'' are 65°S, 38°E; 30°S, 146°E; and 7°S, 18°W, respectively.

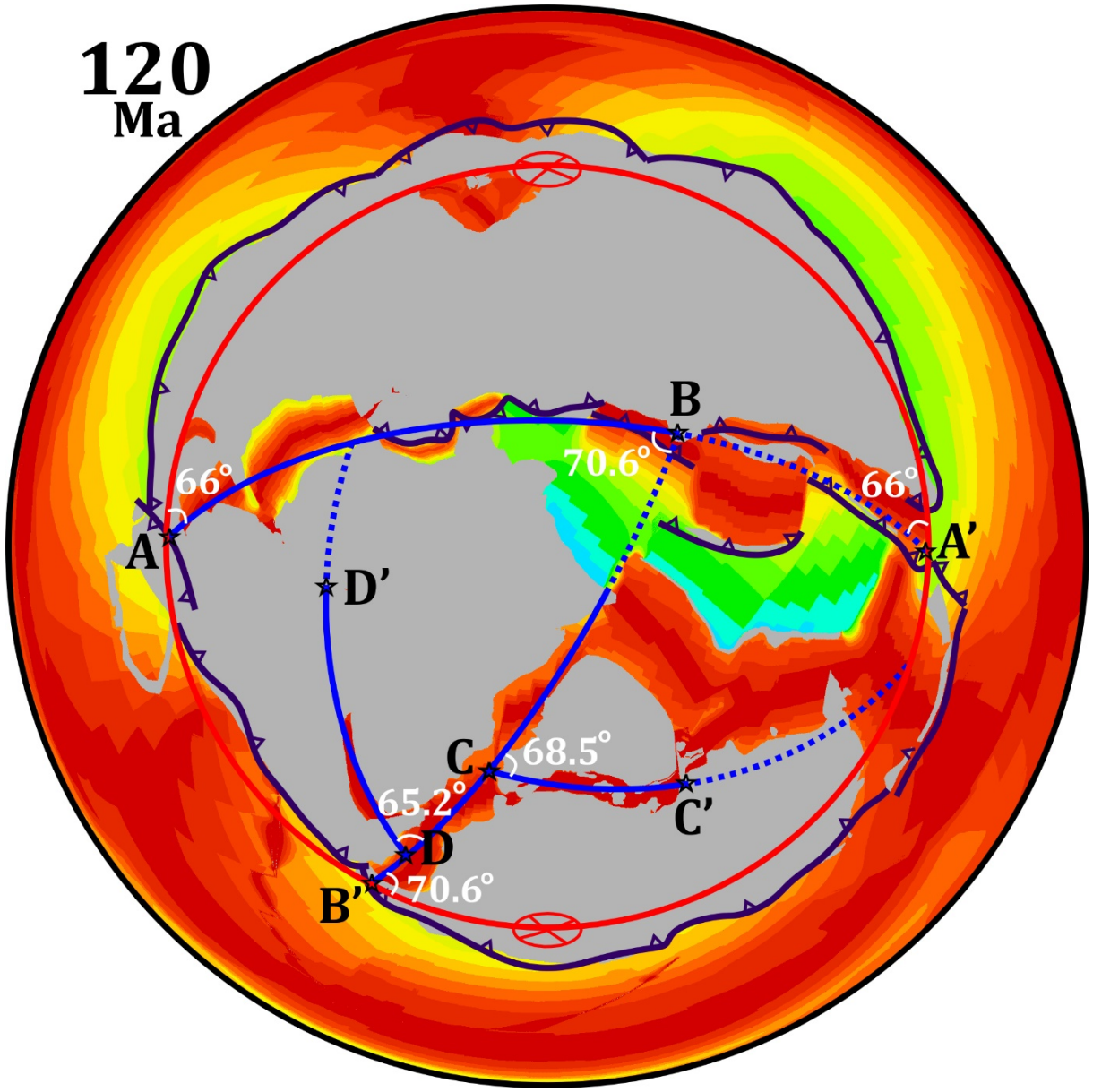

Figure 10. Fracturation of Pangea on 120 Ma reconstruction. Lambert Azimuthal Equal Area projection with pole of projection at 1°N, 34°E. Centers of great circles of AA', BB', CC' and DD' are 62°S, 32°E; 27°S, 141°E; 38°N, 48°E; and 7°S, 76°E, respectively. Note the two new fractures CC' and DD' which appear to be conjugates with respect to fracture B'C.

1. **The 250-140 circular extensional stress phase**

We adjust great circles to the fractures in Figures 9, 10 and 11 to better visualize the evolution of this extensional phase through time and quantify its geometry. The first phase of oscillations at the end of Permian around 250 Ma produced active rifting as well as large flood basalts in Siberia but did not reach the stage of complete continental separation with oceanic formation (Figure 12). On the other hand, the second phase, centered 200 Ma, first opened the Central Atlantic oceanic space about 180 Ma and, by 140 Ma, the counterclockwise of rotation of Laurasia about a pole near point B (Figure 9) had succeeded in opening a continuous oceanic space from the western extremity of the Tethyan realm to the western subduction girdle. It was about 1000 km wide in the future Central Atlantic, somewhat less in the future Caribbean. The great circle ABA' that coincides with the fracture in its western portion passes through the pole of rotation B. Consequently, extension perpendicular to the crack is expected, because the motion of western Gondwana-Land was small as pointed out earlier. The prevailing stress field then was a pure extensional one, the main stress being oriented along small circles with respect to pole B. The great circle ABA' loosely coincides with the southern limit of Laurasia. After 140 Ma, new to young oceanic crust had been put into place along the whole length of AA' and the asthenosphere was close to the surface everywhere. Consequently, stress transmission was not possible any more between Laurasia and Gondwana-Land. Between 140 and 60 Ma, fracturing only affected the former Gondwana-Land.

Consider the second crack that separated Western from Eastern Gondwana-Land after 180 Ma. Eastern Gondwana-Land moved clockwise away from Western Gondwana-Land between 180 and 140 Ma (Figures 7a and 7b). As a result, by 140 Ma (Figure 9), an oceanic space 1500 to 1000 km wide had been opened. The great circle B'B fitted to this crack passes through B that governed the counterclockwise rotation of Laurasia from Western Gondwana-Land. This indicates that, in a first approximation, during this phase, the same homogeneous circular extensional field prevailed over the whole Pangea.

B lies on the limit between the eastern Tethyan realm, north of Eastern Gondwana-Land, and the western one, north of Western Gondwana-Land. Tectonics changed rapidly along AA' on each side of B as the width of the Tethyan realm decreased westward. East of B, shortening along consuming plate boundaries was prevalent whereas west of it, opening along accreting plate boundaries progressively dominated. Trench pull prevailed to the east whereas ridge push increasingly dominated to the west. This had an important consequence. Ridge push and trench pull contributed to the counterclockwise rotation of Laurasia and helped to maintain it. From then on, plate tectonic forces played an increasingly important role in the dynamics of the breakup of Pangea as the sub-Pangea asthenospheric thermal anomaly continuously decreased while the thermal homogenization of the global upper mantle progressed. The change in tectonic style within Neo-Tethys on each side of the northern dotted portion of BB' (Figure 2) explains why reconstructions such as those of Müller et al. (2016, see Figures 3 to 11) needed to introduce along this line an oceanic transform fault.

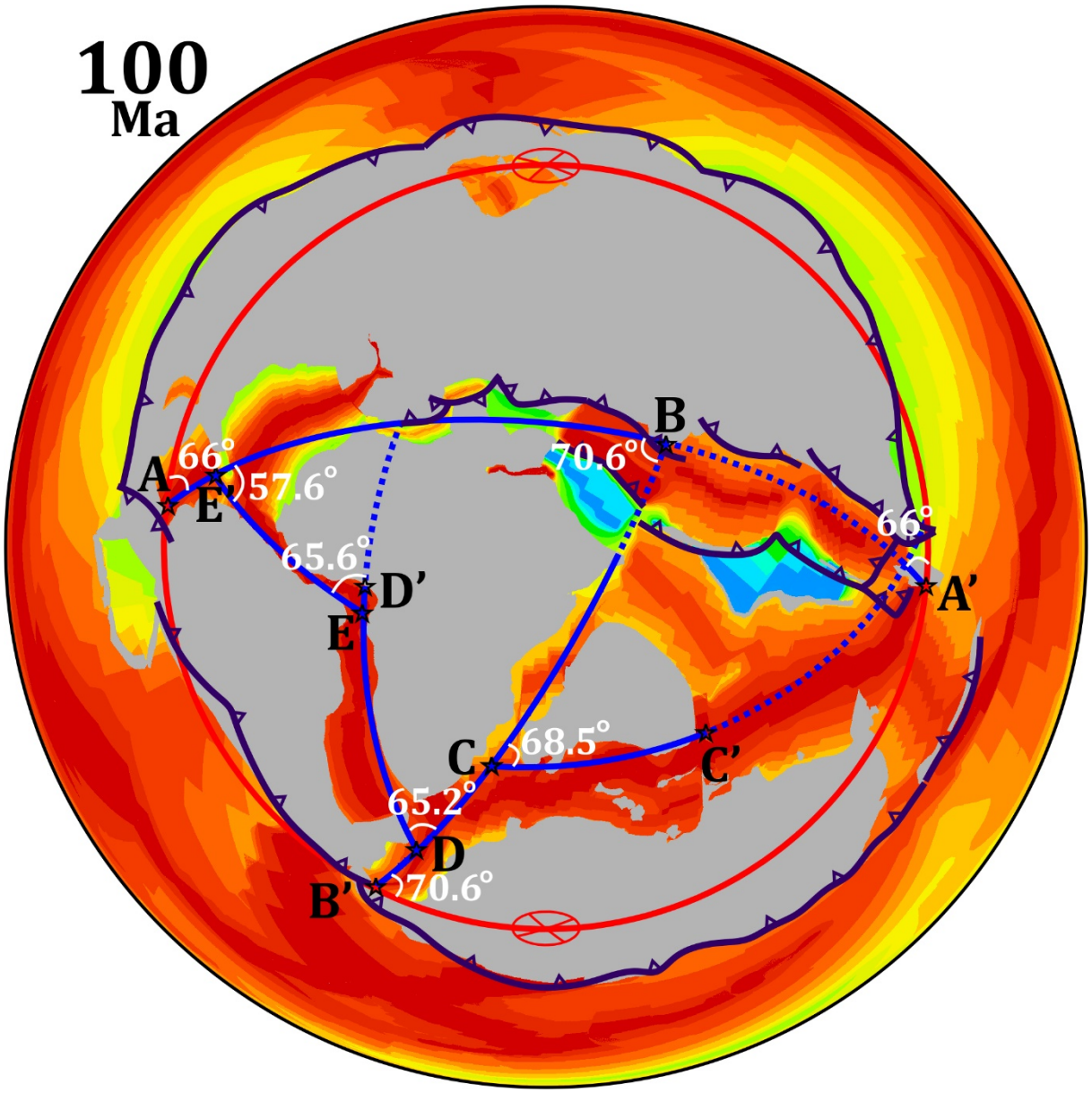

Figure 11. Fracturation of Pangea on 100 Ma reconstruction. Lambert Azimuthal Equal Area projection with pole of projection at 0°N, 32°E. Centers of great circles of AA', BB', CC', DD' and EE' are 63°S, 20°E; 26°S, 138°E; 42°N, 28°E; 9°N, 96°W; and 55°N, 62°E, respectively. The system of fractures, created between 140 and 100 Ma, resembles a flower system with an apex near B' that allows the extension everywhere to be approximately perpendicular to the newly created fractures.

Le Pichon and Huchon (1984) noted that the first large fractures of Pangea that led to oceanization made an angle of about 30° with the perpendicular to the subduction girdle. Because subduction on average must have been frontal around Pangea and consequently induced compressional stresses perpendicular to the subduction girdle, they concluded that these fractures were in the positions of either left or right-lateral shears. We discussed earlier that the presence of such compressional stresses is actually required by the juxtaposition of the warm sub-Pangea asthenosphere with the relatively colder Panthalassa one. And Figures 2 and 9 show indeed that great circles BA and BB' both make an angle of about 25° with the perpendicular to the subduction girdle. They are consequently in position of initial right lateral and left-lateral shears respectively. The 70° angle between great circles AB and B'B suggests that they might be conjugate Coulomb fractures within the lithosphere. We interpret this observation as indicating that the whole thick lithosphere crescent of Pangea acted as a single homogeneous mechanical unit concentrating the stresses that led to the breakup of Pangea. To test further this hypothesis, we have drawn in Figure 9 the great circle BB'', symmetric of BB' with respect to AB, that crosses the area of fracturing that led to the huge 250 Ma flood basalt Siberian event (Ivanov, 2007), (Figures 2, 9 and 12) but failed to form a new ocean. BB'' makes an angle of 70° with BB'. Because, as shown in Figure 12a, the nature and position of the subduction girdle, north of the zone of fracturing, is uncertain, we cannot check the angle of great circle BB'' with it. We feel however that we can conclude that the geometrical configuration of the large fractures indicates that the whole crescent of Pangea acted as a single homogeneous mechanical unit. We will come back later to the 250 Ma extensional and flood basalt event.

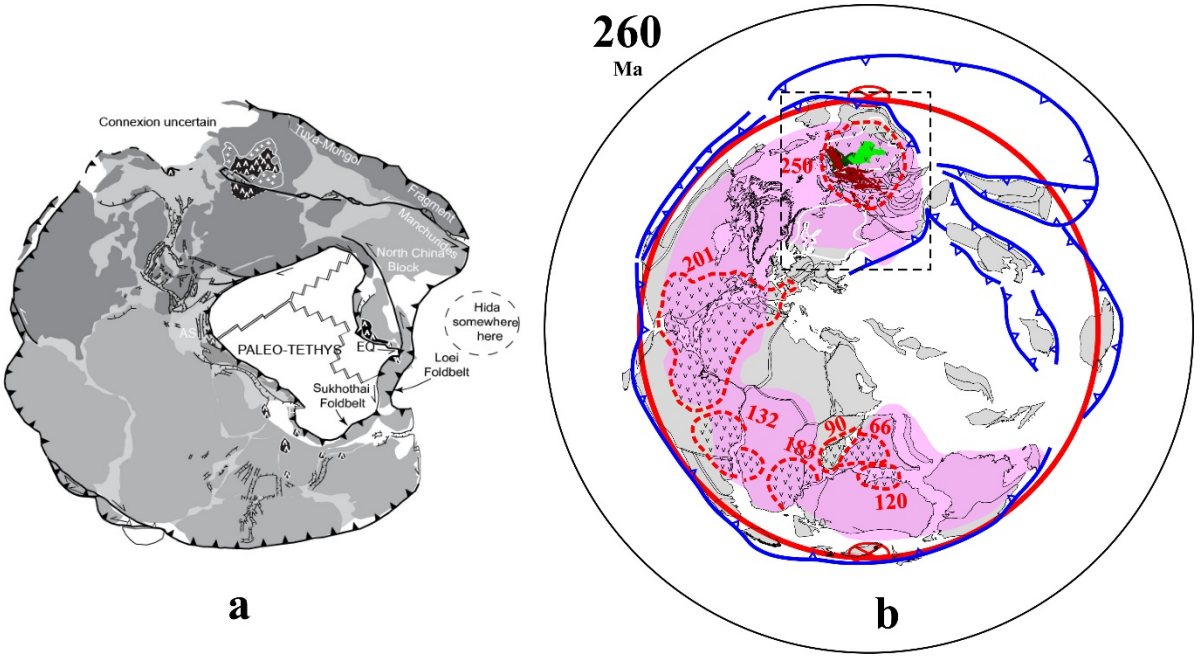

Figure 12. a) Late Permian Pangea (from Le Pichon, Figure 3 modified from Şengör & Atayman, 2009, Figure 15B). Key to symbols: Lines with teeth are subduction zones (teeth on the upper plate), double lines are spreading centers, lines with hachures are normal fault belts (usually delimiting rifts), upsidedown v's are flood basalts (exposed), pluses are flood basalts (covered by younger deposits), half arrows show strike-slip motion. In northern Siberia, data are insufficient to decide on the tectonic regime. b) 260 Ma reconstruction from Domeier & Torsvik (2014). Legends as in Figure 1 with the addition of: - actual mapped volcanics (red, graben volcanics, dark green and light green, flood basalt volcanics) - outlines of cratons in Siberia and Eastern Europe, white lines. Dashed rectangle is the location of the enlargement of Figure 13b.

In summary, during this tectonic phase, Laurasia first moved couterclockwise about point B away from western Gondwana-Land that did not move significantly. Consequently, an oceanic space was created by westward propagation from the western extremity of the Tethyan realm isolating Laurasia from Gondwana-Land. As B did not coincide with the center of Pangea, Laurasia moved slowly outward of the great circle. Eastern Gondwana-Land, 20 Myr later, moved clockwise away from stationary western Gondwana-Land, forming an oceanic space along the thick lithosphere southern portion of B'B. The most remarkable observation though is that the whole Pangea thick lithosphere crescent reacted as a single mechanical unit to a homogeneous stress field. This stress field was purely extensional and the main direction of extension, that we attribute to the oscillations of Pangea about its axis, was oriented along small circles about the axis of symmetry of Pangea. The secondary extension was radial. It was produced by the uplift of the lithosphere pushed upward by the thermally expanding asthenosphere. As the cracks opened and oceanic accretion began to be active, the additional contribution of the plate tectonic forces became increasingly important. Outward of the thick lithosphere crescent, along the peripheral active margin, there was a transition to a compressional stress field, the main compressional direction being radial and perpendicular to the subduction girdle.

1. **The 140-100 Ma extensional fragmentation phase**

We now consider the progress of fracturing between 140 and 100 Ma (Figure 10, 120 Ma and Figure 11, 100 Ma). Between 140 and 120 Ma, two new fractures were formed on opposite side of B'B, initiating the separation of Africa from South America to the west and India from Antarctica-Australasia to the east. The adjusted great circles DD' and CC' both form an angle of 65-70° with the B'B great circle. This observation suggests to us that they are conjugate Coulomb fractures of B'B. These fractures progressively opened because Antarctica-Australasia ceased to move clockwise within Pangea and began instead to pivot counterclockwise with respect to B', producing a circular extensional field about the B' pivot. The stress pattern thus had changed radically, this new extensional field only affecting Gondwana-Land. This rotation, at the difference of the preceding clockwise one, led Antarctica-Australasia to signifi-

cantly infringe on Panthalassa. Note however, that the peripheral subduction margin was still affected by the same compressional field. This might account for the offset of points C and D with respect to B'.

Then, by 100 Ma (Figure 11), the northward rift propagation between South America and Africa had ceased to progress near D' and a new fracture opened along EE', making again an angle of about 65° with the preceding fracture along DD', to form what will become the highly oblique equatorial Atlantic. EE' also makes an angle of about 60° with great circle AB. Figure 11 shows that this new pattern of fractures, created between 140 and 100 Ma, resembles a flower system with an apex in B' that allowed the extension everywhere to be approximately perpendicular to the newly created fractures. As a result, the asthenosphere penetrated widely within the former Gondwana-Land lithosphere. The asthenospheric material came from the gap in the subduction girdle limiting the southeastern Tethyan realm, but also from gaps in the western subduction girdle that were formed in the northern Caribbean near point A and southern Caribbean near point B' (Figures 10 and 11).

1. **Summary of the fracturing phase**

All the fractures we have discussed only occurred within the thick lithosphere crescent (compare Figures 2 and 10, see also Celli et al., 2020). This is strikingly demonstrated when considering the northward progression of the South Atlantic accretionary rift (Figure 11). When the tip of the propagating rift reached what is now the western tip of Brazil, it came out of a thick lithosphere area to enter much thinner African lithosphere. It then immediately bifurcated 65°W to reenter thick lithosphere and begin to form what will become the highly oblique equatorial ocean. This branching configuration is similar to the one obtained with numerical models of propagating rifts imposing a shortening velocity at the tip of the propagator (e.g. Figure 4 of Jourdon et al., 2020).

But why would the deep propagating rift within strong lithosphere resist entering weak lithosphere and chose to bifurcate to reenter strong lithosphere? We consider that this observation confirms our earlier proposition that stresses outside of the strong lithosphere rapidly dissipate within the weak African lithosphere where they produced a complex set of relatively shallow rifts in the Sahara area, whereas stresses were concentrated within the thick lithosphere crescent. The breakup of Pangea then depended on the breakup of the crescent: the rift had to continue to propagate to break the strong crescent and succeed in the breakup of Pangea. We reach the important conclusion that the thick lithosphere crescent was sufficiently strong with respect to the surrounding thin continental lithosphere to react as a single mechanical unit to the uniform stress field. This stress field resulted from the superposition of the effects of the sub-Pangea thermal anomaly of the asthenosphere and of the oscillations of Pangea about its axis.

To summarize, the breakup of Pangea that led to its dispersion was governed exclusively by the fracturing of the strong thick lithospheric crescent. The se-

quence of fracturing was the following: 1) The crescent was broken into three pieces within a circular extensional field. Laurasia moved first counterclockwise about point B and infringed Panthalassa to the north and northwest, followed by east Gondwana-Land which moved clockwise 20 Myr later along the periphery of Pangea. Western Gondwana-Land stayed mostly stationary. 2) Counterclockwise pivoting of eastern Gondwana-Land about its western tip (point B' in Figure 10) produced circular extension centered on B' and fragmentation of the two newly separated pieces of Gondwana-Land. This second generation of cracks produced propagating rifts from D to D' and C to C' (Figures 10, 11). A 65-70° systematic angle related the new generation to the preceding one. The counterclockwise pivoting about B' led to increasing infringing of Gondwana-Land over Panthalassa. It opened a wide opening for asthenosphere transfer between the southeastern Tethyan realm and Panthalassa. 3) The third generation of cracks produced segment D'E' that would join the South Atlantic to the central Atlantic with the same 65-70° branching at both extremities. Consequently, the fracturing was produced in three successive generations. Each generation was related to the preceding one by a simple branching geometry. We propose that each new generation corresponded to Coulomb fractures conjugate of the preceding generation fractures. The 65-70° value of the angle suggests that they propagated within a highly resistant medium. Branching occurred whenever the propagation stalled because of a resistance to propagation. Finally, we suggest that segment BB'' which produced the fracturing leading to the Siberian flood basalt province without ocean creation may belong to the same general pattern of fracturing, as AB is in the position to be a conjugate fracture of BB'' (Figure 2).

The kinematic pattern of breakup just described appears compatible with the simultaneous action of the two extensional forces we discussed in section 2, an outward radial force and an intermittent circular extensional force, although we pointed out that plate tectonic forces, and in particular trench pull and ridge push forces, were also present and played an increasingly important additional role to transfer oceanic space within hemispheric Pangea. However, although widespread extension occurred as soon as the TPW oscillations began in Late Permian, the actual fracturing leading to the formation of new oceanic spaces only began with the second phase of extension about 200 Ma.

The first phase coincided with the fracturing that led to the huge Siberian flood basalts (250 Ma) which failed to completely break apart Laurasia (Figure 2). The second phase coincided first with the fracturing that led to the enormous CAMP flood basalts eruption 201 Ma and then 20 Myr later to the breakup between Western and Eastern Gondwana-Land and the associated Karoo basalts flood basalt eruption (183 Ma, Figure 4). Finally, the third phase, between 140 and 110 Ma, led to major changes in the fracturing pattern of Gondwana-Land as Eastern Gondwana-Land pivoted CCW out of the Pangean hemisphere about its western extremity. This led to fractures between South America and Africa (with the Parana-Etendeka volcanic event, 132 Ma) and then to fractures between India and Antarctica (with the Rajmahal-Shillong-Kerguelen volcanic

events, 118 Ma, Figures 9 and 10).

1. **The consolidation of the thick lithosphere crescent**

   (a) **The thick lithosphere crescent was adjusted to the hemispheric shape of Pangea and homogenized during its accretion**

When considering the tectonics of Pangea, we should be careful that there are three distinct domains (see Figure 12). On the outside of the thick lithosphere crescent identified in Figure 12b in pink, the 1 000 to 2,000-km-wide band of thin lithosphere associated with the peripheral subduction girdle was dominated by subduction related tectonics, as just discussed in the previous section. On the inner side of the lithospheric crescent, the tectonics of the thin and weak continental lithosphere area within the Tethyan realm was controlled by the complex kinematics of the Tethyan oceanic area with its one-way piecemeal transfer of fragments of lithosphere from the south to the north. In between, the resistant thick lithosphere crescent was progressively assembled and consolidated during the accretion phase of Pangea. It is the consolidation of this thick lithosphere crescent that we are considering in this section.

The two Late Permian reconstructions of Figure 12 agree on the configuration of the continuous crescent of thick lithosphere. This is true of most recent reconstructions because of the tight constraints to adjust the thick lithosphere fragments that have since been separated without significant deformation by Pangea disruption. On the other hand, there are significant differences between reconstructions for the outer band associated with the subduction girdle and the thin lithosphere bordering Tethys. The greatest uncertainty concerns the different fragments of eastern Asia still in the process of being accreted.

It is intriguing that, during Permian, the thick lithosphere fragments formed a single continuous crescent adjusted to fit exactly within the hemispheric subduction girdle. This is even more intriguing when we realize that these fragments were continental elements formed much earlier and that, as demonstrated by McKenzie et al. (2015), they ended forming a continuous arc of thick lithosphere (thicker than ~150 km). Yet, they included, beside Archaean and Proterozoic shields, a significant proportion of Paleozoic blocks with no systematic difference in thickness. These observations imply, as proposed by McKenzie et al. (2015) and Priestley et al. (2019), that the forces resisting shortening during the assembly of Pangea were able to homogenize the arc and form a continuous belt of thick lithosphere which, as we have seen above, controlled the fracturing and dispersal of Pangea.

1. **The Late Carboniferous and early Permian consolidation of the northeastern extremity of the crescent**

We now consider, as an enlightening example of this progressive building of the arc, the consolidation of the eastern extremity of the thick lithosphere crescent after the Hercynian suturing of Gondwana and Laurasia during the Late Car-

boniferous and early Permian (Figures 12b and 13). Although orogenic activity persisted further east and southeast well into the Mesozoic, the welding together of the East Siberian Craton (ESC) to the East European craton through the West Siberian Basin (WSB) was in the consolidation process by early Permian (Şengör et al., 1993, 2014). At this time, what is now the WSB was the northwestern extremity of the huge Altaïds orogen and consisted of various tectonic units that had just been accreted together (see Figure 1 of Şengör et al., 2014). By Late Permian, Paleozoic rocks were deeply eroded and, as we will see later, an extensional phase started in late Permian with grabens formation, followed by the formation of a Mesozoic basin, where, outside of the grabens, in most places, the Jurassic is discordant on the much older basement (Ulmishek, 2003). It is thus very surprising that the newly formed lithosphere of the WSB does not appear as a zone of thin lithosphere between the thick lithosphere zones of the two adjacent much older Archean cratons (Figures 12b and 13a). Rather, in the thickness estimates based on S waves of McKenzie et al. (2015), it is occupied by thick lithosphere not significantly different from the adjacent cratons.

Figure 13b shows the present distribution of lithospheric thickness as determined by Priestley and McKenzie (2013). The two Archean cratons (white outlines in Figures 13b) as well as the complex puzzle of blocks that formed the WSB between the two cratons, have a lithosphere thickness larger than 150 km as just stated (blue to green color). Note that the area of thick lithosphere extends further south over the southern Altaïds. These data confirm that the new lithosphere formed during Paleozoic and consolidated during Late Paleozoic acquired a thickness larger than 150 km, not significantly different from the thickness of the adjacent Archean cratons. It seems impossible to escape the conclusion that the new lithosphere was formed as a thick lithosphere during the process of accretion and shortening as proposed by the McKenzie team (Priestley and Debayle, 2003; Priestley and McKenzie, 2006; Priestley and McKenzie, 2013; McKenzie et al., 2015; McKenzie and Priestley, 2016; Priestley et al., 2019), unless the S waves method they used is not reliable.

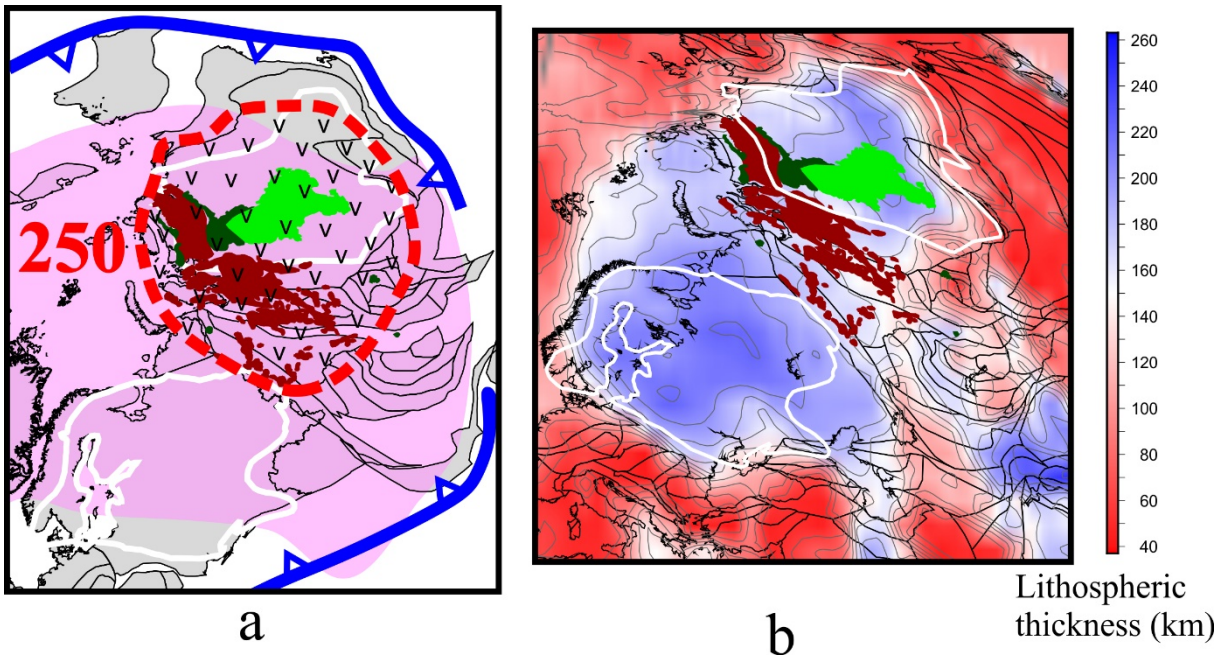

Figure 13. a) Enlarged eastern portion of Figure 12b. Continental borders and contours of blocks used for reconstruction are from Domeier and Torsvik (2014). Note the area of thick lithosphere in pink and the total extent of 250 Ma flood basalt. b) Same eastern Laurasia portion at Present. Pole of projection 4E, 6N with Lambert Azimuthal Equal Area projection (0Ma). Continental borders and contours of blocks as in a).
Actual mapped volcanics (red, graben volcanics, dark green and light green, flood basalt volcanics) and outlines of cratons in Siberia and Eastern Europe, white lines as in Figure 12b. Lithosphere thickness contours and color base from Priestley and Mc Kenzie (2013). From very thin (red and pink) to thick (blue and green). Interval contours 20 km. The West Siberian Basin affected by the orogeny in Paleozoic has acquired a thick lithosphere comparable to the lithosphere of the adjacent cratons.

However, this is one of the best geologically and geophysically studied areas in the world because it is an oil, gas and mineral rich region and the information available there entirely confirms the results coming from the S waves method. A great deal of industrial seismics and commercial drill holes, plus a deep (7.5 km) scientific drill one (SC9) is indeed available there. Long-range P wave profiles have been shot (26 nuclear explosions plus one chemical) (summary in Pavlenkova and Pavlenkova, 2006 for the mantle, Cherepanova et al., 2013 for the crust). Most striking, there is no significant difference between WSB and SC, either in average crustal thickness or in depth to deep mantle reflectors, including the L reflector that is interpreted as the base of the lithosphere. The average crust is 42 km thick in both areas except below the rifts where its

thickness may decrease to 35 km. It has the same velocity of 5.95 km/s. The deep reflectors are continuous from west to east down to the L reflector at a depth near 200 km. The L reflector was identified as the base of the lithosphere because, below it, a large drop in Q factor had been observed, although this observation is disputed. The depth to L decreases toward the south in broad agreement with the S wave solution. Of course, the S waves-based estimates, as well as the long-range P wave profiles, do not resolve features of the order of 100-200 km width. But the average structure is equivalent in terms of average thickness of crust, average velocity of crust, continuity of deep reflectors including L-reflector and depth to isotherm of base of lithosphere based on S waves. We conclude that the lithosphere presently below the WSB acquired its large thickness while it was accreted and consolidated during the second half of the Paleozoic.

As mentioned earlier, this fundamental discovery deeply surprised the McKenzie team. They realized further that world-wide thick continental lithosphere does not systematically coincide with cratonic areas but extend beyond them and sometime stand by themselves as in the case of Tibet and the Iranian plateau zones. We do not discuss here the actual processes of formation of thick lithosphere which are probably among the most interesting problems to solve today in geodynamics. See for example how Klemperer et al (2022) interpret new results on Tibet. But such a discussion is beyond the scope of this paper. We refer the interested reader to the review of Priestley et al (2019). We conclude that the Late Carboniferous and Early Permian consolidation of the eastern extremity of the crescent entirely agrees with the interpretation proposed by McKenzie et al. (2015) and the other papers of this group mentioned above.

1. **The extensional phases that led to the breakup of Pangea**

   (a) **The Late Carboniferous and early Permian first extensional phase**

We now come back to the extensional phases that led to the breakup of Pangea and began during Late Carboniferous and Early Permian. At this time, the axis of symmetry of Pangea had not yet entered the equatorial area and Pangea had not started its oscillations. Consequently, this first phase of extension cannot be related to the oscillations of Pangea about its axis. During this phase of consolidation of the Pangea assembly, rift systems developed in Laurussia over the Variscan and Caledonian belts (Frizon de Lamotte et al., 2015) (see Figure 12a). They have been attributed to the collapse of the high topography of the Caledonian-Variscan belt (Burg et al., 1994). We noted in section 2 that a radial component of extensional stress should have been present within Pangea due to its uplift because of the excess temperature of the asthenosphere below Pangea. The Himalayan topography of these mountain belts obviously increased this extensional stress. This northern rift system joined one along the southwest margin of Tethys that developed behind the subduction of the Paleo-Tethys, as it detached the Cimmerian block and sent it to its northward journey, giving rise to the Neo-Tethys (Şengör et al., 2018). A third branch, perpendicular to

the Tethyan realm extended south across eastern Gondwana, from the Karoo I system to the west, along the eastern border of Africa, to other systems all the way to Antarctica to the east (Frizon de Lamotte et al., 2015). Whatever their causes, all these systems that extended over approximately a whole diameter of Pangea (see Figure 12a) failed to break the thick lithosphere crescent and to produce an oceanic space within it.

1. **The second extensional phase in Late Permian-Early-Triassic during the first oscillation of Pangea**

By about 250 Ma, the first counter-clockwise rotation of Pangea about its axis of symmetry began (Figure 2) as Pangea entered the equatorial zone and this CCW rotation initiated additional circular stresses, as discussed in section 2. Simultaneously, tensional stresses built up in a vast area that extended from Western Europe to Eastern Siberia. Strikingly, the characters of this phase are quite similar both in timing and evolution over this whole area (Nikishin et al., 2002). Rifting began in Late Permian by formation of grabens in which sedimentation was confined. The tectonic subsidence stage extended into the Triassic. It then died out and was followed by thermal subsidence which gave to the basins their bowl shapes, because of the elasticity of the plate and the additional load of sediment. The rifting was accompanied in western Siberia by the huge Siberian flood basalt episode which occurred exactly at the Permo-Triassic boundary (250 Ma, Saunders et al., 2005) (Figures 12b and 13).

The formation of the Paris Basin in Europe occurred during this rifting phase. It has been analyzed in detail by Brunet and Le Pichon (1982) who used the data coming from more than 360 drillings available. Its evolution is remarkably similar to the WSB evolution and gives useful insight into the formation process of these basins. We actually consider the Paris Basin as a reduced model of the WSB, the WSB being 20 times larger in surface and 5 times larger in radius. In what is now the WSB, after Hercynian compression and deformation, Paleozoic rocks were deeply eroded in pre-Triassic. Followed a Late Permian to Early N/S Triassic rift system, depth of rifting increasing rapidly toward the north, and then an undeformed Mesozoic sag that overlied the Hercynian accreted terrane (Ulmishek, 2003; Saunders et al., 2005). Outside of the rifts, in most places, the Jurassic is discordant on the much older basement. There is thus a Permo-Triassic rifting phase, with sedimentation only in the grabens, followed by a post-Triassic thermal subsidence. East of the WSB and north of the SC, rifting extended into the Yenissei-Khatanga Trough during Permo-Triassic (Kontorovich, 2018). And Permo-Triassic extension was also present in the Vilyuy basin to the southeast of the SC (Clarke, 1985). Saunders et al. (2005) suggested that the bulk of basaltic magmatism originated in the rifts to the north, both in the WSB and the Khatanga Trough. They suggested further that the magmas travelled onto the craton either across the land surface, and/or through the crust as dykes or sills.

This extensional phase is in excellent agreement with our proposal that the oscillations of Pangea about itself, as it stabilized within the equatorial zone after its

60° northward migration, created major circular tensional stresses during each reversal. The expected major disruptions in the pattern of stresses happened during the first CCW rotation initiation centered on 250 Ma. This is evidenced by widespread rifting. However, only a few of these rifts succeeded in going into the flood basalt stage and none reached oceanization. We discussed earlier in section 4 the later episodes of fracturing that occurred during the change from CCW to CW centered on 200 Ma and during the progressive change from CW to CCW between 140 and 110 Ma (see Figure 2).

1. **Cretaceous Revolution**

Matthews et al. (2016) have documented a major worldwide plate reorganization between 105 and 100 Ma that is recorded in the stratigraphy by the 100 Ma global-scale unconformity at the Albian-Cenomanian boundary. It marked the passage from Pangea tectonics to contemporaneous plate tectonics and corresponds to what Le Pichon and Huchon (1984) called the Cretaceous Revolution. There is a broad agreement that 100 Ma, at the beginning of Cenomanian, the global sea level had reached a maximum high (Figure 1, Miller et al., 2005; Sneddden and Liu, 2010). This high sea level prevailed until the end of Campanian 70 Ma. It then began to decrease, and this decrease became very large at the beginning of Oligocene, as Eastern Antarctica was covered by a large ice cap. We have argued that, on a long-term time scale, the global sea level was high when the global upper mantle was thermally homogeneous and low when it was thermally isolated. The fact that global sea level had reached its maximum 100-80 Ma would then confirm that the global upper mantle had then been fully homogenized. This reinforces our proposal that the anomalously warm Pangea upper mantle and the oscillations of Pangea about its axis were both key ingredients in the system of forces that fractured Pangea and allowed the homogenization of the global mantle and the dispersal of the separated continents.

The major world-wide plate reorganization described by Matthews et al. (2016) then coincided with the disappearance of the system of forces that fractured the thick lithosphere crescent of Pangea and led to its demise. The Earth had moved from a Buridanian continent system to a modern plate tectonic one. From then on, eastern Antarctica could move freely within Panthalassa. By 60 Ma, Australasia could separate itself from Antarctica and move northward behind the newly created system of marginal basins of what will be the Eastern Pacific (Figures 5 and 6). The continuity of the Pangea subduction girdle had been broken 100 Ma. By 80 Ma, what is now the Pacific side of Antarctica became a passive margin and a 5 000 km gap appeared in the subduction girdle, gap that has been maintained to the Present in the subduction girdle that surrounds the Pacific (Figure 6). The continuous Pacific girdle that was inherited from Pangea was a degraded version of the hemispheric subduction girdle of Pangea but was radically different from its ancestor. The Buridanian continent had ceased to exist.

Figure 11 illustrates how Panthalassa asthenosphere could come through the broad opening of the hemispheric subduction girdle in the southeastern Tethyan

realm and then penetrate within the former Gondwana-Land continent through the newly created flower pattern of fractures with its apex in B'. It is remarkable that this drainage pattern only concerned two thirds of the surface of Pangea as it did not directly reach Laurasia, separated by subduction curtains from Tethys, and as the Atlantic fracturing had not yet propagated within inner Laurasia to create the Arctic Ocean (Figures 5 and 6). However, the relatively recent accretion of eastern Laurasia and its relative isolation behind the northern Tethys subduction curtain might explain why the upper mantle there was not as warm as under most of Pangea. To conclude, the Cretaceous revolution then sealed the demise of Gondwana-Land as a continent.

1. **Discussion and conclusion**

   (a) **Discussion**

      i. **The hemispheric configuration of Pangea**

Le Pichon and Huchon (1984) showed that the outline of Pangea between at least 200 Ma and 125 Ma ago followed exactly a great circle passing through the poles of rotation of the Earth as defined by paleomagnetics. These authors had noted that this polar hemisphere was mostly continental, but not entirely. Le Pichon et al. (2019a) insisted on the fact that the 20% remaining space was not distributed haphazard within the hemisphere. Rather, the whole oceanic space was contained within an equatorial spherical triangle open to the east, the Tethyan realm. Recently Wolf and Evans (2021) demonstrated that this system of polar hemispheric continent surrounded by a subduction girdle with an equatorial Tethyan arm is indeed prevalent in recently published paleogeographic reconstructions for the post-250 Myr Pangea and that this system has essentially been maintained since. However, they confirmed that the subduction girdle was progressively enlarged after the breakup of the continuity of the subduction girdle, as demonstrated earlier in this paper. The existence of this very peculiar system now appears to be established although the actual origins of this configuration of the Tethyan realm and of the near perfect polar hemispheric geometry of Pangea still need to be fully understood.

1. **Absolute reference frame and TPW**

Le Pichon and Huchon (1984), noting that both the present geoid and Pangea had an axis of symmetry in the equatorial plane, assumed that this geometrical configuration was imposed by the pattern of deep convection illustrated by the present geoid and that this pattern was probably sufficiently stable to have been maintained over at least 200 Myr. As a result, both axes of symmetry may have coincided and provided an absolute frame of reference. They then tested whether the hot spot frame of reference reconstructions of Morgan (1981) that extended to 200 Ma agreed with their proposition. They found that the agreement was fair from Present to 80 Ma but a shift of about 20° appeared at 125 Ma and about 30° at 200 Ma. They noted that hot spots are increasingly less constrained prior to 80 Ma and suggested that this might be the cause of this shift. Surprisingly, the situation today on this subject is quite similar (see

Le Pichon for discussion). The difference now is that the reliability of hot spots as an absolute reference frame prior to 80 Ma is increasingly doubted. This is shown for example by the fact that recent search for an optimized absolute reference frame do not use hot spots prior to 80 Ma (Tetley et al., 2019; Müller et al., 2022).

What criterion should then be used prior to 80 Ma? The first one used by these latter authors was to minimize the No Net Rotation (NNR) criterion. Lliboutry (1974) first proposed the No Net Rotation (NNR) condition as an approximation for a reference frame in which the moment of forces acting on the lower mantle is null. Rudolph and Zhong (2014) noted indeed that models with continental keels produce much smaller differential rotation rates between lithosphere and lower mantle than proposed by many absolute motion reference models. Their result, in our opinion, confirms the proposition of Lliboutry that the net rotation of the lithosphere with respect to the lower mantle is negligible and that a good approximation is obtained with NNR. This is quite interesting because the Pangea reference frame gives results quite similar to those of NNR for the Present as well as since the beginning of Mesozoic as noted by Le Pichon et al. (2019a). For example, both frames have small longitudinal motion for South America. This is another argument for the validity of the Pangea frame of reference.

The second criterion these authors used is the minimization of Trench migration rates (this criterion also favored Trench advance). Although they recognized that Van der Meer et al. (2010, 2018) method of relating a trench to a slab gave very useful indications on the motion of the trench with respect to the mantle, they considered that the relation between the slab and trench became too difficult to establish with increasing depth and consequently did not use it. However, in so doing, they lost a powerful constraint in the cases where the continuity can be established. We refer the reader to the discussion by Le Pichon that established the fair agreement of the Trench-Slab method with the Pangea reference frame.

Finally, Müller et al. (2022) noted that their mantle reference frame derived on the basis of the paleomagnetically and geologically derived model of Merdith et al. (2021) is unable to fit properly the 60° northward migration of Pangea that Le Pichon attributed to TPW. They suggested that the reason for the misfit might be that this northward migration was indeed due to TPW. This is a crucial point. If Pangea migrated 60° northward to the equatorial zone through TPW, as proposed by Le Pichon, the question of the formation of LLSVP's is radically changed.

1. **The excess temperature of the asthenosphere below Pangea and sea level change**

   (a) **The excess temperature of the Pangea asthenosphere**

That the asthenosphere below Pangea was at a temperature about 100° to 150°C above the normal potential temperature of about 1350°C was one of the conclu-

sions of Le Pichon. But is this excess temperature established? Lenardic (2017) pointed out that such a transient signal in the cooling rates of the Atlantic and Indian ocean regions compared with the Pacific has indeed be detected (van Avendonk et al., 2017). Le Pichon presented evidence for the existence of such a thermal anomaly below Pangea (Brandl et al., 2013; Kelemen & Holbrook, 1995; Whittaker et al., 2008) and the reader is referred to their discussion. We emphasize here two essential sets of results. First, Brandl et al. (2013) analyzed lavas formed at mid-ocean ridges following continental rifting and break up to obtain contemporaneous upper mantle temperatures over the past 170 Myr. We quote below their essential conclusion. *While samples from the Pacific Ocean do not record raised mantle temperatures, samples from the Atlantic Ocean that formed close to the margin of the rifted continent reveal an upper mantle temperature immediately after continental rifting that was up to 150 °C higher than the present-day average and mantle temperatures remained high for 60–70 Myr.* Second, van Avendonk et al. (2017) compiled oceanic crustal thickness data that spanned ages from Pangea breakup to the present. They connected crustal thickness to mantle temperature at the time of crust formation. Their results showed that the older crust from the Atlantic was unusually thick relative to the modern crust, consistent with a relatively warm mantle below Pangea at the time of its breakup and a progressive dissipation of the Pangea thermal anomaly. In short, the available evidence supports the existence of a 100-150°C temperature anomaly in the upper mantle below Pangea when it started to break apart.

This excess of temperature is of extreme importance for the dynamics of such a Buridanian continent because as emphasized by Lenardic (2017) *supercontinent-induced lateral temperature variation in Earth's mantle is unstable — it can prompt the break-up of a supercontinent, the subsequent drift of continents away from the hot mantle anomaly, and the formation of new ocean basins. Such an anomaly would take over 100 million years to homogenize.* Le Pichon pointed out that the subduction girdle together with the anomalously hot Pangea asthenosphere formed significant mass anomalies which could provide the type of internal mantle loading that Creveling et al. (2012) argued could have driven the TPW event that brought Pangea to the equator (Jellinek et al., 2020; Lenardic et al., 2011). Consequently, a Buridanian continent is by essence a transient feature.

1. **Excess temperature of Pangea asthenosphere and sea level**

We earlier explicitly related this excess temperature to sea level. Unfortunately, quantitative estimations of global sea level variation in the geological record are still affected by large uncertainties (see for example the recent discussion by Van der Meer et al., 2017). An additional difficulty for estimations of sea level during the breakup of Pangea comes from the effect on sea level variations of the excess temperature of the sub-Pangea asthenosphere, effect that is not considered by any of the publications on global sea level record. However, the post-250 Ma qualitative estimates are in fair agreement for the first order trends

shown in Figure 1. This figure, which essentially follows Miller et al. (2005), indicates that the global sea level was high when Pangea started its assembly about 400 Ma, in the early Devonian, that it decreased continuously to a low until the end of Permian (260 Ma). It then started to rise again about 200 Ma, as the fragmentation of Pangea began, to reach a new sea level high about 100 Ma, as Pangea had ceased to exist, indicating that the heating of the Pangea upper mantle had a duration of about 140 Myr whereas the homogenization of the mantle required about 100 Myr. The whole cycle from formation to demise of Pangea had a duration of 300 Myr.

But how well are the dates of beginning and end of the rapid Mesozoic rise of sea level established? We compare in Figure 14 relative variations of sea level after Snedden and Liu (2010) and of flooded continental area after Ronov (as given by Miller et al., 2005) with the relative surface increase of Pangea, based on the Müller et al. (2016) reconstructions between 250 and 80 Ma. The Snedden and Liu curve was recommended to us as the most reliable relative sea level curve by Bill Haq (C.S., personal communication, 2014). There is a consensus among specialists that, as stated by Haq in 2018, "the interval from latest Permian through the earliest Jurassic, a time span of nearly 80 M.y., represents the longest spell of low seastands of the Phanerozoic. " whereas the same author had stated in 2017 that "there was a general rise of sea level through the Jurassic … that began in the early Jurassic, culminating in the peak high in the late Kimmeridgian–early Tithonian interval, before stabilizing in the earliest Cretaceous... ". Figure 14 shows that indeed rapid sea level rise started between 200 and 180 Ma coinciding with breakup that led to the opening of the Central Atlantic. This agrees with Figure 1. In Figure 14, the rate of increase rapidly diminished to reach a plateau near 150 Ma followed by a new slower increase. Maximum sea level was reached in Upper Cretaceous 80 Ma. We conclude that the rapid rise in sea level after a long low sea level stand started about 180 Ma, that the increase slowed significantly about 150 Ma and that the maximum was reached near 100-80 Ma.

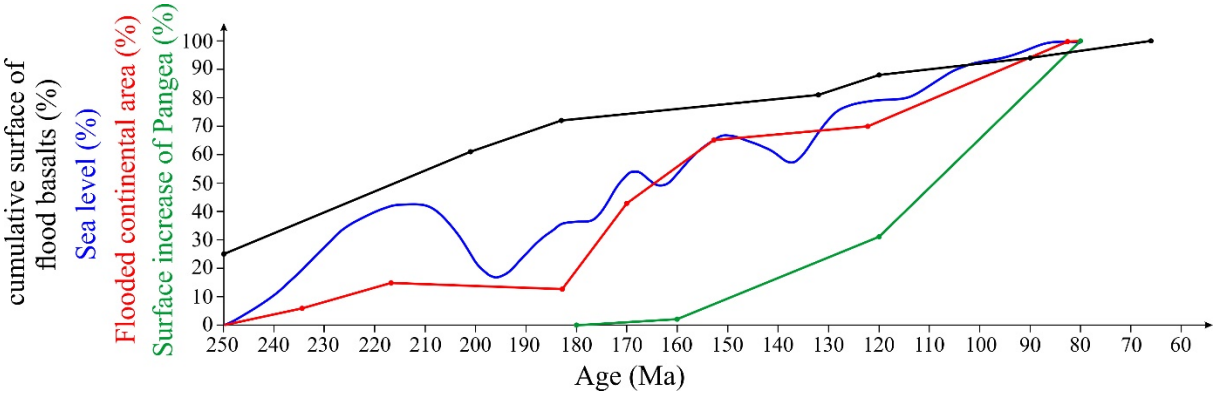

Figure 14. Sea level (blue), flooded continental area (red) and surface increase of Pangea (green) between 250 and 80 Ma. The three curves are given in

percentages between the 250 Ma (0%) and 80 Ma (100%). Sea level after Snedden and Liu (2010), flooded continental area after Ronov (as given by Miller et al. (2005) and surface increase of Pangea, our own estimates based on Müller et al. (2016) reconstructions used in this paper. The cumulative surface of flood basalts between 250 and 66 Ma (black) curve is discussed subsequently in the flood basalts and extension discussion (see text).

The Permo-Triassic low sea level stand thus had a length of about 60 to 80 Myr. This could be interpreted as indicating that the heating of the Pangea upper mantle ceased about 260 Ma and then did not evolve for a length of time of at least 60 Myr. An equilibrium state might have been found leading to a stationary thermal situation. Alternatively, the fact that the change occurred approximately when the 250 Ma Siberian flood basalt province was formed might indicate that this major heat venting was sufficient to interrupt the heating process.

1. **Breakup, excess Pangea asthenosphere temperature and sea level**

We now come back to the third curve of Figure 14 which is our estimate of surface increase of Pangea outward of the great circle based on the Müller et al. (2016) reconstructions. This estimate is of course affected by the uncertainties in the reconstructions. The surface increase of Pangea between 180 and 80 Ma is about 40 M km^2 and is produced by an increase in oceanic area of Pangea. Whereas the rate of increase of sea level curve decreased with time, the rate of increase of surface growth increased with time. This is the paradox we now discuss.

Between 180 Ma and 140 Ma, the growth of Pangea was entirely due to the CCW motion of Laurasia away from Gondwana-Land that was creating the Central Atlantic Ocean and a narrow ocean between Western and Eastern Gondwana-Land but the surface occupied by the Tethys oceanic space did not change. However, 120 Ma, the surface growth had changed radically, as a new CCW rotation of Eastern Gondwana-Land away from Western Gondwana-Land, about a pivot near what will become the southern Antilles, was added to this rotation. As a result, the rate of growth of the surface of Pangea more than doubled. In addition, because Africa and India started moving toward Laurasia, the oceanic Tethys space then started to decrease at the expense of the growing South Atlantic and Indian oceans. This profound dislocation with creation of an oceanic network within the former Gondwana continent cannot be considered any more to be principally the effect of the dissipation of the upper mantle thermal anomaly of Pangea. We pointed out earlier that, as the breakup progressed, plate tectonic forces unleashed by the breakup provided increasingly important additional contributions that finally became dominant.

We showed in section 3 (Figure 7b) that the outgrowth of Pangea was dominated by two main rigid rotations, first of Laurasia (R1), and second of East Gondwana-Land (R2), with their subduction zones attached. R1 opened Gap

1 between Laurasia and South America and Gap2 between West and East Gondwana-Land. R2 opened Gap 3 in Eastern Tethys. The total width of the gaps cannot be more than about one tenth of the total length of the subduction girdle. Looking from the surface, which is the only thing we can do, we conclude that it is through these narrow corridors situated in the southern portion of Pangea that most of the exchange of asthenospheric material between Panthalassa and Pangea could occur. But the exchange concerned the whole upper mantle as the sub-Pangea asthenosphere was separated from the Panthalassa one by the huge slab system extending downward from the surface to at least the base of the upper mantle. And we do not know how the flow of asthenospheric material through these gaps modified the shape of the deep slab curtain. Consequently, we do not know either how the volume of Pangea initially hot asthenospheric material changed with time. Yet the rate of net inflow through the corridors was equal to the net increase of volume of the Pangea asthenosphere. Although the initial force, that exerted the push on the subduction girdle and triggered the rotations of first Laurasia and then East Gondwana-Land, was the excess Pangea upper mantle heat, the plate tectonic forces became increasingly active with time and became dominant as the breakup advanced. Further, the gaps, that were essential in the homogenization process only were an indirect consequence of these rotations.

The global sea level rise was initially very rapid as it had already reached about 65% of its total amount 150 Ma (Figure 14). It was the result of the initial rotation of Laurasia and of the opening of Gap1and Gap2. From then on, and until it reached its maximum 80 Ma, the rise became slower in spite of the addition of the larger opening of Gap 3, presumably because the thermal homogenization was already greatly advanced. The main forces acting on the breakup of Pangea were now the plate tectonic forces. As the homogenization of the global upper mantle temperature progressed, the specificity of the tectonics of Pangea progressively disappeared. By 80 Ma, this homogenization was complete and the Earth had entered into the present plate tectonic system.

Finally, we note that both rotations R1 and R2 were with respect to Western Gondwana-Land which moved least. South America was the only part of Pangea that remained approximately stationary and close to the original location of the subduction girdle. This is intriguing and suggests that the Tethyan oceanic space was a controlling factor in the breakup of Pangea because of its essential role in the evacuation of heat from the mostly continental hemisphere.

1. **The dynamic context**

The factors that make Pangea a unique geologic entity, a true hemispheric supercontinent ringed by a near complete subduction girdle, also make the geodynamics of its break-up unique. The subduction girdle prevents lateral mixing in the mantle, allowing the insulating effect of thick continental lithosphere to become localized – entrained rising plume material could augment sub-Pangea warming related to this effect (Jellinek et al., 2002; Schubert et al., 2004; Davaille, 2018). This leads to a temperature gradient from sub-Pangean to sub-oceanic mantle.

Although other supercontinents may have had subduction girdles, the evidence is less clear and none were of the lateral extent of Pangea; theory, numerical models, and lab experiments have all shown that the insulating potential of a supercontinent depends on its lithospheric thickness and its lateral extent (Lenardic et al., 2011).

A lateral temperature gradient in the mantle will tend to drive mantle flow. Once this gradient becomes sufficiently large, the flow can overcome the strength of the lithosphere and flow resistance from peripheral slabs. This, in turn, will induce a plate driving pulse that will contribute to Pangea breakup (Lenardic, 2016; Le Pichon). This driving force will dissipate as new ocean spreading centers form and as the thermal anomaly spreads with the associated dispersal of continents (Van Avendonk et al., 2016; Lenardic, 2016). As this process evolves and dissipates, more traditional plate tectonic driving forces (ridge push, slab pull, trench suction) will come to play increasingly important roles in breakup. Unlike the spreading of the anomaly, which will have a global character, plate tectonics forces will vary regionally depending on geologic setting. The interaction of the warm anomaly and plate tectonic forces driving breakup reinforces the arguments of Le Pichon et al. (2019) that the character of plate tectonics was radically different between Pangea times and dispersed continental stages. The reconstructions of Pangea breakup, within this contribution, offer a unique constraint on the dynamics of the transient mantle flow component that contributed to Pangea breakup.

The previous section discusses, in detail, how our plate reconstructions can be used to unravel the complex interactions that occur between a global-scale, lateral mantle temperature variation, heterogeneous continental lithosphere, and plate driving forces during Pangea breakup. A useful added exercise, to help constrain the temporal variations between warm spreading mantle and more traditional plate driving forces, is to consider simple models of what breakup and associated sea-level trends would be predicted to be under the assumption that they are due solely to spreading of warm mantle material. The predicted mean trends can then be compared to the actual data trends. Misfits between the two can be used to infer the effects of variable plate driving forces imposed on the pulse of warm spreading mantle.

A lateral temperature gradient will induce buoyancy-driven spread of initially trapped warm sub-Pangean mantle, with associated viscous drag on the lithosphere above and a lateral spread of the subduction girdle. The dynamics of convective flow driven by lateral temperature gradients have been mapped via theory and experiments by Höink et al. (2011). The rate of increase of Pangea surface area (lateral dispersion), and the associated rate of sea level rise, will depend on the spreading speed and on the character of the warm mantle flow. In the limit that spreading occurs as a constant speed channelized flow in response to lateral temperature variations (Hoïnk et al., 2011), the lateral dispersion will increase with time and sea level variations will be proportional to the square of the extent of this flow at any time. If the warm mantle spreads as a low viscos-

ity axisymmetric gravity current against the more viscous surrounding mantle (Griffiths and Campbell, 1991), the lateral dispersion depends on the initial trapped volume and is proportional to time to the $1/5^{th}$ power. Thus, the rate of change of surface area will quickly fall off from an initial maximum. The corresponding sea level rise will evolve as time to the $2/5^{th}$ power and the rate of change will similarly fall off over time. Finally, trying to approximate the N-S polarity of spreading (see above), the low viscosity mantle gravity current might be better approximated as a two-dimensional flow then as an axisymmetric one. In this limit, lateral dispersion will increase as time to the ½ power and the increase in sea level will have the same time-dependence.

From visual inspection of the changes in sea level (Figure 14), the spread of warm mantle occurs in between the two-dimensional and channelized limits. The channelized limit is consistent with rheological arguments that flow will tend to channelize in the upper mantle (Semple and Lenardic, 2017). As previously noted, our expectation was not for a good model fit across the full timing of Pangea breakup. The misfits between the simple model predictions and the data contain information on the temporal trade-offs between different forces that drive Pangea breakup. The spreading model does reasonably well over the time window before 140 Ma but beyond that time frame there are deviations that indicate the enhanced role of traditional plate tectonic driving forces. This is consistent with the dynamic expectation that breakup will lead to the dissipation of the thermal anomaly and a lesser role for it contributing to plate driving forces over time.

A particularly informative deviation, from the simple model prediction, is the fact that the surface area growth of Pangea appears to continuously accelerate from 180-80 Ma (Figure 14). That accelerating trend can be attributed to an enhanced role for slab pull forces which highlights that the effects of a warm mantle anomaly and traditional plate driving forces will be intertwined. More specifically, it has been argued that Pangea formation was associated with a lull in slab flux (Silver and Behn, 2008). This is consistent with dynamic models of super continental insulation (Lenardic et al., 2011). The formation of Pangea, with its subduction girdle, involves continental convergence with associated high slab flux. The development of a thermal anomaly will eventually drive a switch from convergence to dispersal and, along that full path, slab flux should be variable with a low just prior to dispersal. Spreading warm mantle, and tractions on the lithosphere above, can drive the upper continental plate above peripheral subductions zones, which will initiate a pulse of continental arc activity (Lee et al., 2011; Jellinek et al., 2020). It can also trigger enhanced slab flux along peripheral margins which should accelerate over time as mantle flow patterns reconfigure. The predictions that slab pull forces should then increase, as the warm thermal anomaly itself dissipates, are consistent with the general trends of Figure 14 and the more detailed interpretations of the previous section.

1. **The progressive non-uniform enlargement of the subduction girdle**

Our analysis has shown that the subduction girdle did not recede outward uniformly within Panthalassa. Instead, there was a strong polarity in the outward migration. The recession only affected the northern and southern portion whereas the equatorial portion remained unchanged. As a result, the subduction girdle became ellipsoidal with a long axis oriented N20°W-S20°E. We suggest that it is due to the presence of the equatorial Tethyan realm which vented out a great quantity of heat. As the breakup advanced, the role of the eastern Tethyan realm, in direct contact with Panthalassa, became increasingly important and the whole southeastern quadrant of the subduction girdle collapsed. On the other hand, on the opposite side, the southwestern girdle did not recede significantly and remained the part of the girdle that had least moved out. This accounts for the puzzling observation that the subduction opposite South America has moved least since Pangea time.

1. **Plumes did not play a dynamic role in the breakup**

Our kinematic analysis led us to the conclusion that the pattern of breakup of Pangea is not compatible with the hypothesis attributing a major dynamic role to plumes that would have impacted the lower lithosphere. Yet, many authors attribute a major dynamic role to plumes presumably related to these flood basalt provinces that would have impacted the lower lithosphere (e.g. Cande and Stegman, 2011; Van Hinsbergen et al., 2021). As discussed earlier, we do not consider credible the proposition that this highly ordered pattern of fracturing was determined by the locations of the impacts of successive plumes on the lower side of the Pangean lithosphere. Here, we investigate in more detail the association of giant flood basalts provinces with the largest fractures that affected the thick lithosphere shield of Pangea, making its breakup possible.

At the end of section 4, we showed that the totality of the flood basalts provinces related to the breakup of Pangea, from the 250 Ma Siberian province to the 118 Ma Rajmahal-Shillong- Kerguelen provinces, were erupted over thick lithosphere (Figures 2 and 9) and were all related to its progressive fracturing. This is also true of the Madagascar (90 Ma) and Deccan (66 Ma, Figure 9) flood basalts provinces (Bardintzeff et al., 2009; Courtillot and Renne, 2003; Van Hinsbergen et al., 2021) that are not considered in detail in this paper as they occurred after the 100 Ma demise of Pangea. These events occurred 250 to 66 Ma and as a result it is difficult to reconstruct the former extent of the volcanic provinces because of the effect of erosion. The volume of volcanics is even more difficult to estimate. To evaluate the amplitude of these volcanic eruptions, the parameter we choose is the surface that was covered at the time by flood basalts, being aware that this estimate may have large uncertainties. Using this parameter to characterize the succession of these seven flood basalt eruptions, we show in Figure 4 the curve of growth of their cumulative surface. The ages indicated in this paper for flood basalts are now broadly accepted (see Courtillot & Renne, 2003). For the seven events involved, the total cumulative surface is huge, about 28 M km^2, that is about 14% of Pangea continental surface and 22% of the thick lithosphere crescent. The two largest flood basalt provinces are indeed the first

to have been erupted and they both occurred over Laurasia. These are the Siberian flood basalts province (250 Ma) and the CAMP flood basalts province (201 Ma). The first one is related to the unsuccessful fracturing of Laurasia (BB'' fracture of Figures 2 and 9). According to Ivanov (2007), the 250-Ma Siberian trap event, close to the Permo-Triassic boundary, covered about 7 M km^2 (Ivanov, 2007). Courtillot and Renne (2003) simply indicated an original surface larger than 4 M km^2. We adopt the value of 7 proposed by Ivanov (see discussion in Le Pichon et al., 2019). The second flood basalt province, CAMP is related to the first successful fracturing leading to oceanization, near the collision zone of Laurasia and Gondwana (BA fracture in Figures 2 and 9). CAMP is even larger than the Siberian one, although much of its basalt flows are now destroyed by erosion. It is an enormous basalt outpouring that covered both sides of the Central Atlantic rift, extending south over northern Brazil, west to the northern Gulf of Mexico, and north over part of Iberia and France (Marzoli et al., 1999; McHone and Puffer, 2003; Marzoli et al., 2018; Marzen et al., 2020). Courtillot and Renne (2003) estimated the surface as more than 7 M km^2. Marzoli et al. (2018) proposed that the surface was larger than 10, value that we adopt. The western boundary of CAMP coincides with the orogenic axis of the Caledonides, which suggests that this orogenic axis played a role in the localization of the Central Atlantic break. What was by far the main event in this catastrophic set of volcanic eruptions (possibly the largest subaerial flood basalt event ever known) occurred exactly at the Triassic-Jurassic boundary 201 Ma (Marzoli et al., 2011) and its duration was only 600,000 years (Blackburn et al., 2013).

The following flood basalts were significantly smaller as seen on Figures 2 and 9. We adopt for them the values listed by Courtillot and Renne (2003). However, they gave no estimate for Rajmahal-Kerguelen. We adopt for this one the value of 2 M km^2 given by Le Pichon et al. (2019a) on the basis of submarine surveys in the Bay of Bengal. The Karoo flood basalts province (183 Ma, 3.1 M km^2, Jourdan et al., 2007, who proposed an original surface larger than 3.0) is related to the BB' fracture (Figure 9) that was formed when eastern Gondwana-Land started to move clockwise away from western Gondwana-Land while Laurasia was still rotating counterclockwise. The next two provinces were produced during the extensive fracturing pattern of Gondwana between 140 and 110 Ma. The Parana-Etendeka volcanic province (132 Ma, 2.3 M km^2, Jourdan et al., 2007) is associated with the DD' fracturing whereas the Rajmahal-Shillong-Kerguelen volcanic province (118 Ma, Kent et al., 2002, 2.0 M km^2) is associated with the CC' fracture. As just mentioned above, we do not discuss in this paper the 90 Ma Madagascar (1.6 M km2, Bardintzeff et al., 2009) and the 66 Ma Deccan (1.8 M km^2, Courtillot and Renne, 2003) flood basalt provinces produced during the following dispersal phase of Pangea but note that these four volcanic provinces, from Parana-Etendeka to Deccan, as the three previous ones, occurred over thick Pangea lithosphere and are related to fractures of thick lithosphere.

The first three provinces are associated with fractures BB'', BA and BB' produced by Rotation R1 (Figure 2). We have related them to the initiation (250

Ma) and reversal (200 Ma) of the first CCW oscillation of Pangea (see Figure 1) and have shown that they were created by the same circular extensional field about the pole of rotation R1 (Figure 7). The first two fractures affected Laurasia and the third one Gondwana-Land. These three provinces are the three largest, especially if one takes into account that the estimate we adopted for Karoo surface is considered to be an underestimate (Jourdan et al., 2007).

The youngest four provinces are associated with intra Gondwana-Land fractures produced during Rotation R2 (Figure 7). The first two are the Parana-Etendeka volcanic province (Figure 10) associated with the DD' fracture and the the Rajmahal-Kerguelen volcanic province (Figure 10) associated with the CC' fracture. The last two provinces are associated with later fractures that occurred during the separation of India from Madagascar, producing first the Madagascar province (Figure 4) and then the Deccan province (Figure 5). Their average surface is about 2 M km^2/Myr, three times less than the three first provinces erupted during the first extensional phase (R1). It is tempting to relate the difference in size between these two groups to the large excess temperature of the asthenosphere between 250 and 183 Ma whereas this excess was mostly dissipated when the other four volcanic provinces were erupted during Cretaceous, as testified by the sea level curve of Figure 4. This 100-150°C excess temperature implied a larger amount of partial fusion that could be tapped when the opening of the fractures enabled the ascent of magma within the crust.

Coming back to the cumulative surface of flood basalts curve of Figure 14, it is intriguing that the volcanic provinces related to these two successive rotations R1 and R2 define two rectilinear segments. The first one, between 250 Ma and 183 Ma (Triassic to Lower Jurassic) has a slope of about 0.2 M km^2/Myr and the second one, between 183 Ma and 66 Ma (Middle Jurassic to Cretaceous) has a slope about three times smaller of about 0.06 km^2/Myr. Taken at face value, these might be a measure of the production rates of the sources of magma tapped by these two successive extensional phases. However, although the linearity of the last four data points may be more than a coincidence, the linearity of the first three data points is extremely fragile and we do not wish to speculate about their possible significance. We conclude that massive flood volcanism was widely associated with the fracturing of the thick lithosphere crescent of Pangea (note however that this association was not systematic as flood basalts are not found over the whole length of all the fractures). Figure 4 demonstrates further that the intensity of flood volcanism was about three times larger during the initial fracturing phase (R1) than during the later one (R2). We attribute this difference to the homogenization of the upper mantle temperature produced by Pangea breakup that led to the progressive elimination of the 100-150°C excess temperature in the upper mantle below Pangea. Figure 4 shows that by 140 Ma two thirds of the sea level rise had already occurred, indicating that a corresponding proportion of the excess temperature had disappeared.

Why then no large flood basalt eruption affected the thin lithosphere area, in particular the area situated southwest of the Tethyan realm? A first explanation

comes from the fact that the flood volcanism occurred along the major fractures that broke the crescent within which the stresses had been concentrated as discussed earlier. But the eastern part of fracture BA (Figure 9) extended within the thin lithosphere of the western peri-Tethyan area where extensional tectonics and volcanism were widespread during Upper Triassic all the way to Anatolia and the Levant area (see Le Pichon et al., 2018, 2019) and yet no flood basalt occurred there. In section 1, we have shown that the thickness of the lithosphere of Pangea progressively increased from very little at the crest of the ridge within the Tethyan realm to more than 150 km below the thick cold surrounding continental lithospheric crescent. The base of the lithosphere thus formed a funnel shape opening to the east that could act as a large escape hatch where heat and magma could easily vent out to be evacuated through the accreting boundaries of the Tethyan realm.

In this context, one would expect flood basalt then not to correspond to typical hot (>1500°C and up to 1600°C) plume volcanics but to have been the result of long time mixing between plume and anomalously hot mantle material within the asthenosphere. Jourdan et al. (2007) pointed out that the major flood basalt outpouring in most cases preceded the beginning of seafloor spreading by only a few millions of years and in a few cases (e.g., Deccan) may have been coeval with it but that this relatively brief event was the outcome of a long preparatory phase of extension that extended over up to tens of millions of years. Marzoli et al. (2018) concluded an extensive synthesis on the CAMP Province by stating that a contribution from a deep mantle-plume is possible but not required by geochemical and thermometric data. They concluded further that CAMP basalts indicate temperatures of 1430°C-1480°C. This is the temperature we expect in the Pangea upper mantle. It is significantly lower than temperatures expected for plume-related LIPs as stated above. We feel that the existing data comfort our conclusion.

We conclude that it is probably next to impossible to relate a flood basalt province over thick lithosphere to a hot spot source whereas hot spot trails over thin oceanic lithosphere are easy to detect and much more reliable to use for evaluation of relative motion with respect to the possible hot spot source. In this context, it is interesting to consider what happens in the transition from an opening fracture that had produced flood basalts to the new oceanic floor. Le Pichon et al. (2019 a) noted that a remarkable character of the Indian and South Atlantic Oceans is the presence of large volcanic ridges and massifs in continuity with the emerged magmatic provinces. These outpourings of basalt are often aligned along fractures parallel to flow lines of the opening and they tend to decrease in width with time (Sheth, 1999). This suggests that the rifting-apart led to continuous tapping of the huge asthenospheric reservoir through privileged fractures connected to the new accreting boundary.

1. **Conclusion**

We have investigated the kinematics and dynamics of the breakup of Pangea between 200 and 100 Ma. We have linked them to the continuous rise of sea

level from a Triassic low to an Upper Cretaceous maximum. We argue that the rise in sea level reflects the progressive thermal homogenization of the global upper mantle as the subduction girdle lost its capacity to insulate due to its breakup.

The forces resisting shortening during the assembly of Pangea were able to form and homogenize a continuous crescent of thick lithosphere which acted as an armor and controlled the fracturing and dispersal of Pangea. The crescent concentrated the stresses and acted as a stress guide. This is because stresses rapidly dissipated within the equatorial Tethyan oceanic realm and its adjacent thin lithosphere areas. The base of the lithosphere further formed a funnel opening to the east and hot asthenospheric material was evacuated toward the Tethyan oceanic realm that acted as a large escape hatch.

Our analysis of kinematics demonstrates that Pangea was first elongated by about 3000 km in a NNW-SSE direction and that the length of the subduction girdle increased by about 5000 km. This lengthening occurred mostly through the formation of three new gaps in the subduction girdle opposite what will become the Northern and Southern Caribbean on the west side and a new southeast Tethyan realm opening on the east side.

The analysis of the mechanics of fracturing shows that the breakup of Pangea was governed exclusively by the fracturing of the strong thick lithospheric crescent that concentrated the stresses. The highly ordered pattern of fracturing was produced through three successive generations, each generation related to the preceding one by a simple branching geometry. Each new generation appears to correspond to Coulomb fractures conjugate of the preceding generation fractures. The 65-70° value of the angle suggests that they propagated within a highly resistant medium. By 100 Ma, the asthenospheric material had been able to widely penetrate within the former Gondwana-Land, mostly from a large gap in the subduction girdle in the southeastern Tethyan realm. The transgression then reached its peak, indicating that thermal homogenization of the upper mantle had been completed. The Earth had entered the Cretaceous Revolution (Le Pichon and Huchon, 1984) that passed from Pangea tectonics to contemporaneous plate tectonics. It was accompanied by a major worldwide plate reorganization between 105 and 100 Ma marked in the stratigraphy by the 100 Ma global-scale unconformity at the Albian-Cenomanian boundary (Matthews et al., 2016).

We noted that major flood basalt provinces that occurred during the breakup of Pangea were associated with fractures that had affected the thick lithosphere crescent. We proposed that the crescent lithosphere of Pangea, that could not be broken by plumes, first had to be fully fractured by major tectonic forces before massive magmatic eruptions could occur. We attribute these tectonic forces to the oscillations of Pangea as it entered the equatorial zone.

Finally, the study we just presented reinforces the concluding statement made by Le Pichon that Present plate tectonics cannot account for Pangea tectonics.

This is because the fact that the supercontinent is constrained to fit within a single hemisphere, with only 20% ocean surface, is a powerful, and potentially unique kinematic constraint. Connecting Pangea breakup to the effects of a subduction girdle adds a dynamic component as the lateral thermal anomaly that develops in the mantle, due to a subduction girdle, generates a transient plate-driving force that contributes to Pangea breakup and dissipates subsequently (Lenardic, 2017). Thus, not only are geologically recent plate kinematic inferences not extendable into the Cretaceous, but neither are mantle dynamic and associated planetary cooling inferences.

Data Availability Statement

There are no new data. Data all come from publications: Le Pichon et al. (2019a), Lenardic et al. (2011), Müller et al. (2016), Domeier and Torsvik (2014), Miller et al. (2005), Torsvik et al. (2012), Van der Meer et al. (2010), Şengör and Atayman (2009). They are listed in the references and cited in the text.

References

Anderson, D. L. (1982). Hot spots, polar wander, Mesozoic convection and the geoid. *Nature*, *297*(5865), 391–393. https://doi.org/10.1038/ 297391a0

Anderson, D. L. (1994). The sublithospheric mantle as a source of continental flood basalts: The case against the continental lithosphere and plume head reservoirs. *Earth and Planetary Science Letters*, *123*(1-3), 269–280. https://doi.org/10.1016/0012-821X(94)90273-9

Bardintzeff, J. -M., Liégeois, J. –P., Bonin, B., Bellon, H., & Rasamimanana, G. (2009). Madagascar volcanic provinces linked to the Gondwana break-up: Geochemical and isotopic evidences for contrasting mantle sources. *Gondwana Research, 18*(2-3), 295-314. https://doi.org/10.1016/j.gr.2009.11.010

Blackburn, T. J., Olsen, P. E., Bowring, S. A., McLean, N. M., Kent, D. V., Puffer, J., et al. (2013). nZircon U-Pb Geochronology Links the End-Triassic Extinction with the Central Atlantic Magmatic Province. *Science, 340*(6135), 941-945. https://doi.org/10.1126/science.1234204

Brandl, P. A., Regelous, M., Beier, C., & Haase, K. M. (2013). High mantle temperatures following rifting caused by continental insulation. *Nature Geoscience, 6*, 391–394. https://doi.org/10.1038/ngeo1758

Brunet, M. F., & Le Pichon, X. (1982). Subsidence of the Paris Basin. *Journal of Geophysical Research: Solid Earth, 87*(B10), 8547-8560. https://doi.org/10.1029/JB087iB10p08547

Burg, J. P., Van den Driessche, J., & Brun, J. P. (1994). Syn- to post-thickening extension in the Variscan Belt of western Europe: Modes and structural consequences, *Géologie de la France,* (3), 33–51.

Cande, S. C., & Stegman, D. R. (2011). Indian and African plate motions

driven by the push force of the Reunion plume head. *Nature, 475*, 47-52. https://doi.org/10.1038/nature10174.

Cawood, P. A., Hawkesworth, C. J., & Dhuime, B. (2013). The continental record and the generation of continental crust. *Bulletin of the Geological Society of America, 125*(1-2), 14–32. https://doi.org/10.1130/B30722.1

Celli, N. L., Lebedev, S., Schaeffer, A. J., Ravenna, M., & Gaina, C. (2020). The upper mantle beneath the South Atlantic Ocean, South America and Africa from waveform tomography with massive data sets. *Geophysical Journal International, 221*(1), 178–204. https://doi.org/10.1093/gji/ggz574

Cherepanova, Y, Artemieva, I. M., Thybo, H., & Chemia, Z. (2013). Crustal structure of the Siberian craton and the West Siberian basin: An appraisal of existing seismic data. *Tectonophysics, 609*, 154–183. http://doi.org/10.1016/j.tecto.2013.05.004

Clarke, J. W. (1985). *Petroleum geology of East Siberia* (Open-File Report 85-367). US Geological Survey.

Coltice, N., Bertrand, H., Rey, P., Jourdan, F., Phillips, B. R., & Ricard, Y. (2009). Global warming of the mantle beneath continents back to the Archean. *Gondwana Research*, *15*(3-4), 254–266. https://doi.org/10.1016/j.Gr.2008.10.001

Coltice, N., Phillips, B. R., Bertrand, H., Ricard, Y., & Rey, P. (2007). Global warming of the mantle at the origin of flood basalts over supercontinents. *Geology*, *35*(5), 391–394. https://doi.org/10.1130/G23240A.1

Courtillot, V. E., & Renne, P. R. (2003). On the ages of flood basalt events. *Comptes Rendus Geoscience*, *335*(1), 113–140. https://doi.org/10.1016/S1631-0713(03)00006-3

Creveling, J. R., Mitrovica, J. X., Chan, N.-H., Latychev, K., & Matsuyama, I. (2012). Mechanisms for oscillatory true polar wander. *Nature*, *491*(7423), 244–248. https://doi.org/10.1038/nature11571

Davaille, A. (2018). Structure of mantle convection: Plumes and plates. Fifty years of Plate Tectonics, then, now and beyond, Collège de France, Paris, June 25–26. https://www.college-de-france.fr/site/barbara-romanowicz/symposium-2017-2018_1.htm

Domeier, M., & Torsvik, T. H. (2014). Plate tectonics in the late Paleozoic. *Geoscience Frontiers*, *5*(3), 303–350. https://doi.org/10.1016/j.gsf.2014.01.002

Du Toit, A. L. (1937). *Our wandering continents*. London: Oliver and Boyd.

Elsasser, W. M., 1967. *Convection and stress propagation in the upper mantle* (Tech. Rept., 5, 23 pp.) Princeton Univ. (reprinted in S.K. Runcorn (ed.), *The application of Modern Physics to the Earth and Planetary Interiors*, (1969, 223-246). Wiley, New York.)

Frizon de Lamotte, D., Fourdan, B., Leleu, S., Leparmentier, F., & De Clarens, P. (2015). Style of rifting and the stages of Pangea breakup. *Tectonics*, *34*(5), 1009–1029. https://doi.org/10.1002/2014TC003760

Griffiths, R. W., & Campbell, I. H. (1991). Interaction of mantle plume heads with the Earth's surface and onset of small-scale convection. *Journal of Geophysical Research: Solid Earth, 96*(B11), 18295-18310. https://doi.org/10.1029/91JB01897

Haq, B. U. (2018). Triassic eustatic variations reexamined. *GSA Today, 28*(12), 4-9. https://doi.org/10.1130/GSATG381A.1

Haq, B. U. (2017). Jurassic Sea-Level Variations: A Reappraisal. *GSA Today*, *28*(1), 4-10. https://doi.org/10.1130/GSATG359A.1

Höink, T., Jellinek, A. M., & Lenardic, A. (2011). Viscous coupling at the lithosphere-asthenosphere boundary. *Geochemistry, Geophysics, Geosystems, 12*(10), Q0AK02. https://doi.org/10.1029/2011GC003698

Ivanov, A. V. (2007). Evaluation of different models for the origin of the Siberian traps. *Special Paper Geological Society of America*, *430*, 669–691. https://doi.org/10.1130/2007.2430(31)

Jellinek, A. M., Gonnermann, H. M., & Richards, M. A. (2002). Plume capture by divergent plate motions: Implications for the distribution of hotspots, geochemistry of mid-ocean ridge basalts, and estimates of the heat flux at the core-mantle boundary. *Earth and Planetary Science Letters*, *205*(3-4), 361-378. https://doi.org/10.1016/S0012-821X(02)01070-1

Jellinek, A. M., Lenardic, A., & Pierrehumbert, R. T. (2020). Ice, Fire, or Fizzle: The Climate Footprint of Earth's Supercontinental Cycles. *Geochemistry, Geophysics, Geosystems*, *21*(2), e2019GC00846. https://doi.org/10.1029/2019GC008464

Jourdan, F., Féraud, G., Bertrand, H., & Watkeys, M. K. (2007). From flood basalts to the inception of oceanization, Example from the 40Ar/ 39Ar high-resolution picture of the Karoo large igneous province. *Geochemistry, Geophysics, Geosystems*, *8*(2), Q02002. https://doi.org/10.1029/2006GC001392

Jourdon, A., Le Pourhiet, L., Mouthereau, F., & May, D. (2020). Modes of propagation of continental breakup and associated oblique rift structures. *Journal of Geophysical Research: Solid Earth*, *125*(9), e2020JB01990. https://doi.org/10.1029/2020JB019906

Keidel, J. (1916). La geología de las sierras de la Província de Buenos Aires y sus relaciones con las montañas de Sud Africa y los Andes. *Buenos Aires: Annales del ministerio de Agricultura de la Nacíon, Sección Geología, Mineralogía y Minería, 3*, 1–78.

Kelemen, P. B., & Holbrook, W. S. (1995). Origin of thick, high-velocity igneous crust along the U.S. East Coast Margin. *Journal of Geophysical Research: Solid Earth*, *100*(B6), 10077–10094. https://doi.org/10.1029/95JB00924

Kent, R. W., Pringle, M. S., Müller, R. D., Saunders, A. D., & Ghose, N. C. (2002). 40Ar/39Ar geochronology of the Rajmahal basalts, India and their

relationship to the Kerguelen Plateau. *Journal of Petrology*, *43*(7), 1141–1153. https://doi.org/10.1093/petrology/43.7.1141

Kontorovich, V. A., Kalinin, A. U., Kalinina, L. M., Solovev, M. V., & Guseva, S. M. (2018). Seismogeological characteristics and oil-and-gas content of the Kara Sea shelf (South Kara, North Kara sedimentary basins). *IOP Conf. Ser.: Earth Environmental Science, 193*, 012032.

Klemperer, S. L., Zhao, P., Whyte, C. J., Darrah, T. H., Crossey, L. J., Karlstrom, K. E., et al. (2022). Limited underthrusting of India below Tibet: $^{3}H/^{4}H$ analysis of thermal springs locates the mantle suture in continental collision, *Proceedings of the National Academy of Sciences of the United States of America*, *119*(12), e2113877119. https://doi.org/10/1073/pnas.2113877119

Lee, C. -T. A., Luffi, P., & Chin, E. J. (2011). Building and destroying continental mantle. *Annual Review of Earth and Planetary Sciences, 39*(1), 59-90. https://doi.org/10.1146/annurev-earth-040610-133505

Lenardic, A., Moresi, L., Jellinek, A. M., O'Neill, C. J., Cooper, C. M., & Lee, C. T. (2011). Continents, supercontinents, mantle thermal mixing, and mantle thermal isolation: Theory, numerical simulations, and laboratory experiments. *Geochemistry, Geophysics, Geosystems*, *12*(10), Q10016. https://doi.org/10.1029/2011GC003663

Lenardic, A. (2017). A supercontinental boost. *Nature Geoscience*, *10*(1), 4–5. https://doi.org/10.1038/ngeo2862

Le Pichon, X., & Huchon, P. (1983). Pangée, géoïde et convection. *Comptes rendus de l'Académie des Sciences*, *296*(II), 1313–1320.

Le Pichon, X., & Huchon, P. (1984). Geoid, Pangea and convection. *Earth and Planetary Science Letters*, *67*(1), 123–135. https://doi. org/10.1016/0012-821X(84)90044-X

Le Pichon, X., Şengör, A. M. C., & İmren, C. (2019a). Pangea and the lower mantle. *Tectonics*, *38*(10), 3479–3504. https://doi.org/10.1029/2018TC005445

Le Pichon, X., Şengör, A. M. C., & İmren, C. (2019b). A new approach to the opening of the Eastern Mediterranean Sea and the origin of the Hellenic Subduction Zone. Part 1: The Eastern Mediterranean Sea. *Canadian Journal of Earth Sciences*, *56*(11), 1119-1143. https://doi.org/10.1139/cjes- 2018-0128

Le Pichon, X., Jellinek, M., Lenardic, A., Şengör, A. M. C., & İmren, C. (2021). Pangea Migration, *Tectonics*, *40*(6), e2020TC00658. https://doi.org/10-1029/2020TC006585

Lliboutry, L. (1974). Plate movement relative to rigid lower mantle. *Nature*, *250*(5464), 298–300. https://doi.org/10.1038/250298a0

Marzen, R. E., Shillington, D. J., Lizarralde, D., Knapp, J. H., Heffner, D. M., Davis, J. K., & Harder, S.H. (2020), Limited and localized magmatism in the

Central Atlantic Magmatic Province. *Nature Communications, 11*(3397), 1-8. https://doi.org/10.1038/s41467-020-17193-6

Marzoli, A., Callegaro, S., Dal Corso, J., Davies, J. H. F. L., Chiaradia, M., Youbi, N., et al. (2018). The Central Atlantic Magmatic Province (CAMP): a review. In L.H. Tanner (Ed.), *The Late Triassic World* (TGBI, Vol. 46, pp. 91-125). Springer International Publishing. https://doi.org/10.1007/978-3-319-68009-5_4

Marzoli, A., Jourdan F., Puffer J. H., Cupone, T., Tanner L. H., Weems, R.E., et al. (2011). Timing and duration of the Central Atlantic magmatic province in the Newark and Culpeper basins, eastern U.S.A. *Lithos, 122*(3-4), 175-188. https://doi.org/10.1016/j.lithos.2010.12.013

Marzoli, A., Renne, P. R., Piccirillo, E. M., Ernesto, M., Bellieni, G., & De Min, A. (1999). Extensive 200 million-year-old continental flood basalts of the Central Atlantic Magmatic Province. *Science*, *284*(5414), 616–618. https://doi.org/10.1126/science.284.5414.616

Matthews, K. J., Seton, M., & Müller, R. D. (2016). A global plate reorganization event at 105–100 Ma. *Earth and Planetary Science Letters*, *355–356*, 283–298. https://doi.org/10.12016/epsl.2012.08.023

McHone, J. G., & Puffer, J. H. (2003). Flood basalt provinces of the Pangean Atlantic Rift: Regional extent and environmental significance. In P. M. Le Tourneau & P. E. Olsen (Eds.), *The Great Rift Valleys of Pangea in Eastern North America* (Chap. 10, pp. 141–154). Volume 1: Tectonics, Structure, and Volcanism, Columbia University Press New York. https://doi.org/10.7312/leto11162-009

McKenzie, D. (2020). The structure of the lithosphere and upper mantle beneath the Eastern Mediterranean and the Middle East. *Mediterranean Geoscience Reviews, 2*, 311–326. https://doi.org/10.1007/s42990-020-00038-1

McKenzie, D., Daly, M. C., & Priestley, K. (2015). The lithospheric structure of Pangea. *Geology*, *43*(9), 783–786. https://doi.org/10.1130/ G36819.1

McKenzie, D. & Priestley, K. (2008). The influence of lithospheric thickness variations on continental evolution. *Lithos, 102*(1-2), 1-11. https://doi.org/10.1016/j.lithos.2007.05.005

McKenzie, D. & Priestley, K. (2016). Speculations on the formation of cratons and cratonic basins. *Earth and Planetary Science Letters, 435*, 94–104. http://dx.doi.org/10.1016/j.epsl.2015.12.010

Merdith, A., S., Williams, S. E., Collins, A. S., Tetley, M. G., Mulder, J. A., Blades, M. L., et al. (2021). Extending full-plate tectonic models into deep time: Linking the Neoproterozoic and the Phanerozoic, *Earth-Science Reviews*, *214*, 103477. https://doi.org/10.1016/j.earscirev.2020.103477

Miller, K. G., Kominz, M. A., Browning, J. V., Wright, J. D., Mountain, G. S.,

Katz, M. E., et al. (2005). The Phanerozoic record of global sea-level change. *Science*, *310*(5752), 1293–1298. https://doi.org/10.1126/science.1116412

Morgan, W. J. (1981). Hotspot tracks and the opening of the Atlantic and Indian Oceans. In C. Emiliani (Ed.), *The Sea* (7, pp. 443-487). J. Wiley and Sons, New York, N.Y. https://doi.org/10.1016/0040-1951(83)90013-6

Müller, R. D., Cannon, J., Tetley, M., Williams, S. E., Cao, X., Flament, N., et al. (2022). A tectonic-rules based mantle reference frame since 1 billion years ago – implications for supercontinent cycles and plate-mantle system evolution. *Solid Earth Discussions, EGU.* https://doi.org/10.5194/se-2021-154

Müller, R. D., Seton, M., Zahirovic, S., Williams, S. E., Matthews, K. J., Wright, N. M., et al. (2016). Ocean basin evolution and global-scale plate reorganization events since Pangea breakup. *Annual Review of Earth and Planetary Sciences*, *44*(1), 107–138. https://doi.org/10.1146/annurev-earth-0600115-012211

Nikishin, A. M., Ziegler, P. A., Abbott, D., Brunet, M. F., & Cloetingh, S. (2002). Permo-Triassic intraplatemagmatism and rifting in Eurasia: implications for mantle plumes and mantle dynamics. *Tectonophysics, 351*(1-2), 3-39. https://doi.org/10.1016/S0040-1951(02)00123-3

Pavlenkova, G. A., & Pavlenkova, N. I. (2006). Upper mantle structure of the Northern Eurasia from peaceful nuclear explosion data. *Tectonophysics, 416*(1-4), 33–52. https://doi.org/10.1016/j.tecto.2005.11.010

Paulsen, T., Deering, C., Sliwinski, J., Chatterjee, S., & Bachman, O. (2022). Continental magmatism and uplift as the primary driver for first-order oceanic $^{87}Sr/^{86}Sr$ variability with implications for global climate and atmospheric oxygenation. *GSA Today*, *32*(2), 4-10. https://doi.org/10.1130/GSATG526A.1.CC-BY-NC.

Priestley, K., & Debayle, E. (2003). Seismic evidence for a moderately thick lithosphere beneath the Siberian Platform. *Geophysical Research Letters, 30*(3), 1118. https://doi.org/10.1029/2002GL015931

Priestley, K., & McKenzie, D. (2006). The thermal structure of the lithosphere from shear wave velocities. *Earth and Planetary Science Letters, 244*(1-2), 285–301. https://doi.org/10.1016/j.epsl.2006.01.008

Priestley, K., & McKenzie, D. (2013). The relationship between shear wave velocity, temperature, attenuation and viscosity in the shallow part of the mantle. *Earth and Planetary Science Letters, 381*, 78–91. https://doi.org/10.1016/j.epsl.2013.08.022.

Priestley, K., McKenzie, D., & Ho, T. (2019). The lithosphere-asthenosphere boundary-a global model derived from multimode surface- wave tomography and petrology. In H. Yuan, B. Romanowicz (Eds.), *Lithospheric discontinuities, geophysical monograph* (Vol 239, pp. 111-123). American Geophysics Union. The lithospheric thickness model is available from http://ds.iris.edu/ds/products/emc- cam2016/(file CAM2016Litho.tgz)

Rudolph, M. L., & Zhong, S. J. (2014). History and dynamics of net rotation of the mantle and lithosphere. *Geochemistry, Geophysics, Geosystems*, *15*(9), 3645–3657. https://doi.org/10.1002/2014GC005457

Saunders, A. D., England, R. W., Reichow, M. K., & White, R. V. (2005). A mantle plume origin for the Siberian traps: uplift and extension in the West Siberian Basin, Russia. *Lithos, 79*(3-4), 407–424. https://doi.org/10.1016/j.lithos.2004.09.010

Schubert, G., Masters, G., Olson, P., & Tackley, P. (2004). Superplumes or plume clusters?. *Physics of the Earth and Planetary Interiors*, *146*(1-2), 147-162. https://doi.org/10.1016/j.pepi.2003.09.025

Semple, A.G., & Lenardic A. (2018). Plug flow in the Earth's asthenosphere. *Earth and Planetary Science Letters, 496*, 29-36. https://doi.org/10.1016/j.epsl.2018.05.030

Şengör, A. M. C., & Atayman, S. (2009). The Permian extinction and the Tethys: An exercise in global geology. *Geological Society of America Special Paper, 448*, x+96. https://doi.org/10.1130/2009.2448

Şengör, A. M. C., Lom, N., Zabcı, C., Sunal, G., & Öner, T. (2021). The Saharides: Turkic-type orogeny in Afro-Arabia. *International Journal of Earth Sciences.* https://doi.org/10.1007/s00531-021-02063-3

Şengör, A. M. C., Natal'in, B.A., & Burtman, V.S. (1993). Evolution of the Alataid tectonic collage and Palaezoic growth in Eurasia. *Nature, 364*, 299-307. https://doi.org/ 10.1038/364299a0

Şengör, A. M. C., Natal'in, B.A., Van der Voo, R., & Sunal, G. (2014). A new look at the Altaids: a superorogenic complex in northern and central Asia as a factory of continental crust. Part II: Paleomagnetic data, reconstructions, crustal growth and global sea-level. *Austrian Journal of Earth Sciences, 107*(2), 131-181.

Şengör, A. M. C., Natal'in, B.A., Van der Voo, R., & Sunal, G. (2018). The tectonics of the Alataids: crustal growth during the construction of the continental lithosphere of Central Asia between 750 M and 130 Ma ago. *Annual Review of Earth and Planetary Sciences, 46*, 439–494. https://doi.org/10.1146/annurev-earth-060313-054826

Sheth, H. C. (1999). Flood basalts and large igneous provinces from deep mantle plumes: Fact, fiction and fallacy. *Tectonophysics*, *311*(1-4), 1–29. https://doi.org/10.1016/S0040-1951(99)00150-X

Silver, P.G., & Beher, M.D. (2008). Intermittent Plate Tectonics. *Science, 319*(5859), 85-88. https://doi.org/10.1128/science.1148397

Snedden, J. W., & Liu, C. (2010). *A compilation of Phanerozoic sea-level change, coastal onlaps and recommended sequence designations* (Search and discovery, Article ID. 40594). Online H-Journal for E&P Geoscientists.

Steinberger, B., & Torsvik, T. H. (2008). Absolute plate motions and true polar wander in the absence of hotspot tracks. *Nature*, *452*(7187), 620–623. https://doi.org/10.1038/nature06824.PMID/18385737

Tetley, M. G., Williams, S. E., Gurnis, M., Flament, N., & Müller, R. D. (2019). Constraining absolute plate motions since the Triassic. *Journal of Geophysical Research: Solid Earth*, *124*(7), 7231–7258. https://doi.org/10.1029/2019JB017442

Torsvik, T. H., Van der Voo, R., Preeden, U., Mac Niocaill, C., Steinberger, B., Doubrovine, P. V., et al. (2012). Phanerozoic polar wander, palaeogeography and dynamics. *Earth-Science Reviews*, *114*(3–4), 325–368. https://doi.org/10.1016/j.earscirev.2012.06.007

Ulmishek, G. F. (2003). *Petroleum geology and resources of the West Siberian Basin, Russia* (Rep. 20201-G). US Geological Survey Bulletin.

Van Avendonk, H. J. A., Davis, J. K., Harding, J. L., & Lawver, L. A. (2017). Decrease in oceanic crustal thickness since the breakup of Pangaea. *Nature Geoscience*, *10*(1), 58–61. https://doi.org/10.1038/ngeo2849

Van der Meer, D. G., Spakman, W., Van Hinsbergen, D. J. J., Amaru, M. L., & Torsvik, T. H. (2010). Towards absolute plate motions constrained by lower-mantle slab remnants. *Nature Geoscience, 3*(1), 36–40. https://doi.org/10.1038/ngeo708

Van der Meer, D. G., Van den Berg van Saparoea, A. P. H., Van Hinsbergen, D. J. J., Van de Weg, R. M. B., Godderis, Y., Le Hir, G., & Donnadieu, Y. (2017). Reconstructing first order changes in se level during Phanerozoic and Neoproterozoic using strontium isotopes. *Gondwana Research, 44, 22-34.* https://doi.org/10.1016/j.gr.2016.11.002

Van der Meer, D. G., Van Hinsbergen, D. J. J., & Spakman, W. (2018). Atlas of the underworld: Slab remnants in the mantle, their sinking history, and a new outlook on lower mantle viscosity. *Tectonophysics*, *723*, 309–448. https://doi.org/10.1016/j.tecto.2017.10.004

Van Hinsbergen, D., Steinberger, B., Guilmette, C., Maffione, M., Gürer, D., Peters, K., et al. (2021). A record of plume-induced plate rotation triggering sea-floor spreading and subduction initiation. *Nature Geoscience, 14*, 626-630. https://doi.org/10.1038/S41561-021-00780-7

White, R. S., & McKenzie, D. (1995). Mantle plumes and flood basalts. *Journal of Geophysical Research*, *100*(B9), 17543–17585. https://doi.org/10.1029/95JB01585

Whittaker, J. M., Müller, R. D., Roest, W. R., Wessel, P., & Smith, W. H. F. (2008). How supercontinents and superoceans affect seafloor roughness. *Nature*, *456*(7224), 938–941. https://doi.org/10.1038/nature07573

Wolf, J., & Evans, D. A. D. (2021). Reconciling supercontinent cycle models with ancient subduction zones. *Earth and Planetary Science Letters, 578*, 117293. htpps://doi.org/10.1016/j.epsl2021.117293

Zhong, S., Zhang, N., Li, Z. X., & Roberts, J. H. (2007). Supercontinent cycles, true polar wander, and very long wave-length mantle convection. *Earth and Planetary Science Letters*, *261*(3-4), 551–564. https://doi.org/10.1016/j.epsl.2007.07049